Programmed Temperature Electrospray Ionization (ptESI) for Thermal Cycling of Proteins

May Anna Constabel

A thesis

submitted in partial fulfillment of the

requirements for the degree of

Master of Science

University of Washington

2024

Committee:

Matthew F. Bush

Nicholas M. Riley

Program Authorized to Offer Degree:

Applied Chemical Science and Technology

University of Washington

Abstract

Programmed Temperature Electrospray Ionization (ptESI) for Thermal Cycling of Proteins

May Anna Constabel

Chair of the Supervisory Committee:

Matthew F. Bush

Department of Chemistry

Temperature-controlled electrospray ionization (tcESI) coupled to mass spectrometry (MS) gives detailed structural information of proteins and has been used to study their thermal denaturation. In this work, our programmed-temperature electrospray ionization (ptESI) source is used to rapidly heat and cool a nanoESI capillary containing proteins in solution. The structural changes of acidified ubiquitin and lysozyme are investigated during both unfolding and refolding. ptESI uses fast scan rates, allowing for short experiment times, and results in data dense experiments. As mass spectra are acquired continuously while temperature is scanned. Both ubiquitin and lysozyme exhibited highly reversible unfolding and refolding at different scan rates, but only lysozyme displayed a scan rate dependence; the midpoint temperatures (T_m) shift to higher temperatures with increasing scan rates. This scan-rate dependence indicates the

unfolding and refolding transitions are not at equilibrium and there is a partial kinetic component. The refolding of lysozyme appears to be frustrated as there is a large difference between the unfolding and refolding curves and midpoint temperatures (ΔT_m). ΔT_m also displays a scan-rate dependence, as it increases with increasing scan rate. This research demonstrates that ptESI can be used to determine T_m values, probe protein unfolding and refolding, and reveal kinetic dependencies for reversible transitions. Based on these results, I propose that ptESI can be used to investigate protein stability and scan-rate dependence in protein folding studies, in binding or thermostability assays, and can be a valuable tool for studying biomolecules.

ACKNOWLEDGEMENTS

I would like to first thank my advisor, Dr. Matt Bush, for his guidance over the course of my research. His knowledge and insight have been invaluable. I will always be grateful for his enthusiasm, advice, and support. I would like to thank Dr. Nick Riley for sitting on my thesis committee. I would also like to thank Dr. Meagan Gadzuk-Shea and acknowledge her work designing and building the ptESI source.

I must thank every member of the Bush lab for their support, suggestions, discussions, and friendship. I would especially like to thank Chris, for the endless conversations, time spent in lab, joint problem solving, and jokes; Dr. Theresa Gozzo, who has now graduated, for training me on native mass spectrometry, the instrumentation, and other lab skills I needed to succeed; Addison, for the wonderful discussions about our research and beyond; and Carley, for helping me collect data and teaching me how to be a better mentor by being an amazing mentee.

I am deeply grateful for all the friends I made in Seattle, especially those in the Chemistry Department and on the Husky Cycling team. I also want to thank all my friends in Vancouver who encouraged me to take the leap and go back to school.

Finally, I would like to thank my parents, Peter and Lynn, my little brother Kai, and my boyfriend Graham for their advice, encouragement, and love over these past 18 months.

TABLE OF CONTENTS

ACKNOWLEDGEMENTS 5

TABLE OF CONTENTS 6

CHAPTER I 8

Introduction 8

References 18

CHAPTER II 27

Evaluating the Reversible Unfolding of Ubiquitin and Lysozyme at Low pH Using Programmed Temperature ESI (ptESI) 27

Introduction 27

Materials and Methods 29

Results and Discussion 30

Conclusions 46

Acknowledgements 47

References 48

CHAPTER III 57

Conclusions 57

References 61

APPENDIX A 70

Supplemental Information for Chapter III 70

References 86

CHAPTER I

Introduction

Anfinsen's dogma states that the native structure of a protein is unique, the most thermodynamically stable, and arises from the polypeptide primary structure through folding.[1] The importance of protein folding is becoming more and more emphasized as we begin understand the link between misfolded proteins and disease, however, the actual process of folding remains only partially understood. It is difficult to study protein folding *in vivo*, as the cell is a crowded and concentrated environment. Though the *in vitro* environment does not fully reflect *in vivo* conditions, *in vitro* folding is easier to reproduce and control.[2] Model proteins, like ubiquitin and lysozyme, are used due to their small size, fast folding rate and now their long history of study.[2] The simplest way to study protein folding is to start with the folded protein, perturb the native structure, and study the subsequent refolding. Several different methods can be used to perturb protein structure, either alone or in combination: chemical denaturants, pH, reducing agents, pressure, and temperature have commonly been used.[3] Out of these methods, temperature is a convenient denaturation strategy that does not require solution additives and is a "universal factor of influence with a fundamental physical meaning".[4]

Traditional Methods for Characterizing Protein Stability

Previously, thermal studies of protein folding have mostly relied on calorimetric or optical methods like differential scanning calorimetry (DSC), differential scanning fluorescence (DSF), and circular dichroism (CD). DSC measures the difference between a reference and a sample cell as the temperature of both cells is increased. DSC can operate across the wide

temperature ranges over which changes in protein structure can occur. It is also highly stable and sensitive technique.[5] DSC has been used in protein thermal denaturation studies for many years and is still the method of choice for precisely determining thermodynamic parameters for protein unfolding. Changes in molar heat capacity, enthalpy of unfolding, and melting temperature related to unfolding events are determined directly and can be used to calculate the Gibbs free energy of the transition.[6] Heat capacity is plotted against temperature and unfolding events are characterized as strong peaks. The heat capacity for the specific transition is the magnitude of the unfolding peak, the enthalpy is determined by the total area under the peak, and the melting temperature is the temperature at which the unfolding peak has a maximum.[6] Comparing the heat capacity and the enthalpy gives a measure of the cooperativity of the transition.[7]

In DSC, to test if an unfolding event is reversible or not, the sample is cooled to the starting temperature and scanned again. If no peak is visible on the second scan, it is deemed an irreversible transition. This measure of irreversibility is a simple metric that may be useful for simple system; the thermal denaturation of proteins is often a complex transition that is represented only by a single peak in DSC. It is also limited by slow scan rates, often 0.1 – 2.5 $^{\circ}C \cdot min^{-1}$, resulting in long experiment times, It may also introduce the problem of aggregation at elevated temperatures, as the exposed hydrophobic residues of unfolded proteins interact and aggregate in an irreversible, thermodynamically favourable process.[4] DSC requires large amounts of concentrated sample,[5] which may be difficult to obtain or express for some proteins. It is also very low throughput, as a single experimental run often takes many hours and only a single sample can be run at a time.[5] At low pH, the protein sample is often dissolved in buffer with dilute glycerol added as a stabilizer, but this may affect intermolecular interactions and has been found to shift native protein structures to more compact states.[8] Fast scanning calorimetry

(FSC) has been developed as a faster version of DSC. It uses ultrafast scan rates of 600 – 2400 $^{\circ}C \cdot min^{-1}$, allowing for shorter experiment times and can help avoid aggregation effects.[9] FSC requires smaller sample volumes than DSC, however samples are also often prepared in glycerol solutions to minimize the effect of evaporation due to the low sample volume.[9,10]

DSF, often commonly called fluorescent thermal shift assay (FTSA), uses a fluorescent dye that emits light in non-polar environments, such as the hydrophobic regions in proteins. As the temperature increases, the protein unfolds and the dye interacts with the exposed hydrophobic core.[11] The intensity of the fluorescence is measured as temperature is scanned. DSF has been gaining popularity for use in thermal stability experiments, ligand binding experiments, and drug screening assays in the pharmaceutical industry.[11] It is particularly useful as a broad screening assay as it is target-independent.[11] DSF is commonly run on real-time PCR instruments in multi-well plates, allowing for high-throughput experiments and small sample volumes. The interactions between protein and dye will vary depending on their respective chemical structures, thus the dye must be carefully selected, as some protein and dye pairs may not result in a detectable transition.[12] One of the most commonly used dyes, SYPRO Orange, is favoured because of its high signal-to-noise ratio,[13] but it is proprietary and has no available structural information, limiting the understanding of potential interactions with proteins.[5] The dye is added in large excess, often up to 20-fold. This can perturb the equilibrium of the system as the dye binds to the protein through Le Chatelier's principle, and could introduce errors in some thermodynamic binding assays.[11] Furthermore, experiments in the absence of protein show that the intensity of fluorescence often decreases with increasing temperature,[14] which may complicate analysis. Proteins with many accessible tryptophan and tyrosine residues are likely to have high background fluorescence, as the dye will associate before the protein has unfolded.[11]

Unlike DSC, DSF cannot measure direct thermodynamic values like enthalpy, but a midpoint transition temperature (T_m) can be determined by the inflection point of the curve or the midpoint of the fluorescence transition after a baseline approximation.[12] Changes in T_m can be compared as an measure of stability, but cannot be converted into physiologically relevant thermodynamic parameters or binding affinities.[11]

CD measures the difference in absorption of left- and right-handed circularly polarized light through an asymmetric structural feature, resulting in elliptically polarized light. The α-helices and ß-sheets in folded proteins have characteristic CD spectra at specific wavelengths, giving a direct measurement of protein secondary structure.[15] Far-UV CD is extremely sensitive to the protein backbone and its conformation.[16] Near-UV CD is sensitive to aromatic amino acid side chains and can be indicative of tertiary structural elements.[17] As the temperature increases and the protein unfolds, these structural elements begin to be lost and the changes in ellipticity are measured. Some CD instruments are capable of ramping temperature, though most require setting specific temperature points and equilibration times, and collecting individual spectra at these temperatures.[15] Spectra must be collected at several wavelengths, so taking CD measurements over a range of temperatures becomes time-consuming. It is estimated that collecting initial spectra at a single wavelength will take 7 – 8 hours, and an unfolding and refolding experiment will take 12 – 14 hours.[15] The spectra collected must then be deconvoluted to determine what fraction of folded states are contributing to the spectra. Although CD is primarily a structure-focused method, thermodynamics of unfolding can also be estimated through the change in the fraction of folded states with temperature.[15]

These traditional thermal techniques work well when we assume simple unfolding transitions are occurring in simple solution conditions. Multiplexing is generally not possible as

the signal from individual proteins cannot be separated, and the readout is an average measurement of the mixture. In both DSC and DSF, there is a documented dependence of T_m on scan rate.[10,12,18,19] While it is more commonly known that irreversible transitions have scan rate dependence, it was found that the apparent T_m also increases with increasing scan rate for reversible transitions.[18] This suggests that reversible protein transitions may be partially kinetically controlled. The folding of small proteins is thought to be on the order of microseconds to seconds,[2] so it is commonly assumed that the protein is at equilibrium throughout a thermal unfolding experiment, especially at the low scan rates used in DSC. Though thermal scanning CD instruments exist, there is no record of scan rate dependence in CD experiments.

Models for Protein Folding

Ubiquitin is a highly conserved protein across eukaryotes involved in many cellular processes and disfunction has been linked to several diseases.[20] It is commonly used as a model protein as it is small, has a very structured native conformation and is stable across a broad range of pHs.[21] It has been studied using many different techniques resulting in extensive stability work and one of the most complete pictures of a folding energetic landscape.[21] The T_m of ubiquitin can be shifted to lower temperatures by lowering the solution pH.[22]

Hen-egg white lysozyme (referred to as lysozyme from here on) is another one of the most extensively studied proteins and has been used as a model system for protein folding as well. Many of these studies have probed lysozyme folding at low pH, as the structure is very stable near neutral pH and must be perturbed further to induce a transition between 0 – 100 ˚C.[23]

Studies have shown that lysozyme remains very stable in acidic conditions and the structure remains similar to that at native pH, though the rates of unfolding and folding are slower.[24,25]

MS Methods for Characterizing Protein Stability

Since the advent of native mass spectrometry (MS), in which ions are generated by electrospray ionization of biomolecules prepared in aqueous solutions with physiologically relevant pH and ionic strength, there have been efforts to control the temperatures of liquid samples and probe the stability of non-covalent complexes in solution.[26] Mass spectrometry provides more detailed structural information compared to the traditional techniques and can also give information on molecular events that occur during transitions.[27] One of the earliest temperature-controlled sources designed used a chrome wire wrapped around ceramic block containing an electrospray capillary.[28] Now, most devices use a Peltier thermoelectric chip that controls the temperature of a metal block. For example, one such design was used to study the equilibria of oligomeric states of the small heat shock protein TaHSP16.9.[29] Many of these sources use protocols where the desired temperature is set, the source and capillary must then equilibrate for 1 – 10 min, then mass spectra are acquired for several minutes before this is all repeated at the next temperature increment.[29,30,27,31–35] This results in time-consuming experiments and few data points across the transition. Other source designs are capable of ramping the temperature, at rates of 1 – 5 ˚C·min^{-1},[36–38] resulting in shorter experiment times and continuous measurements. The fastest reported scan rate is 240 ˚C·min^{-1}, though it was recommended to scan at more moderate rates that do not exceed the rate of mass spectral acquisition.[39]

There is no set name for the field, so it will be referred to here as tcESI. The many source designs have been given many different names, such as temperature-controlled ESI (TC-ESI),[29,40,30,27,36,37] variable-temperature ESI (vt-ESI),[31,41,35,42] and digital temperature control ESI (DTC-ESI),[39] among other unnamed sources. Recently, a laser has been used to heat the liquid at the tip of an electrospray emitter, allowing for the accurate determination of melting curves on a timescale of seconds.[43] The laser-heated ESI (LH-ESI) heats only a small volume of liquid, so molecules could diffuse in and out of the laser-heated area during electrospray.

Average charge state is the most common metric to characterize protein unfolding using MS. As the protein unfolds with increasing temperature, more protonation sites become accessible and the charge state distribution shifts to higher charge states. tcESI data is often represented as plots of average charge state versus temperature. The unfolding is visible as a sigmoidal transition with the inflection point of the curve fit giving the T_m. Alternatively, native and unfolded charge state distributions can be established, and the tcESI data represented as the relative abundance of the two fractions versus temperature.[39] In these types of plots, T_m is determined by the intersection of the curve for the native and unfolded fractions.

Both ubiquitin and lysozyme have previously been studied using tcESI, but the refolding of both proteins has been less well investigated. El-Baba and coworkers identified intermediate conformations of ubiquitin using ion mobility-MS and probed the effect of buffers on its stability at low pH.[33] The reversibility of ubiquitin unfolding was tested by incubating the solution at 90 ˚C before cooling to 26 ˚C and analyzing the sample. It was found to be reversible as the spectrum was indistinguishable from a sample that had not been incubated[33], but the transition that occurred during cooling was not measured. In a follow-up study, the tcESI temperature profile was reversed and revealed a similar curve[35], but the data and curve are not shown. In one

of the earliest tcESI studies, Benesch and coworkers documents the unfolding of lysozyme at pH 2.[29] They compared the T_m determined by tcESI with the T_m determined by fluorescence measurements and found good agreement, concluding that this technique gives accurate determinations of T_m and can be used to study thermal effects on proteins.[29] Wang and coworkers repeated these lysozyme unfolding experiments with their own source and were able to replicate the results.[27] However, they link the appearance of high charge states to disulfide scrambling, in which the native disulfide bonds are broken and do not reform resulting in irreversible unfolding. However, it seems the refolding was not investigated and whether this is indeed irreversible is not fully evaluated. This dissertation will test the hypothesis that native disulfide bonds are broken during tcESI experiments.

ptESI Source Background and Description

The programmed temperature nanoESI (ptESI) source in its current iteration was designed and built in 2020 by Dr. Meagan Gadzuk-Shea, a former student in the group, who performed successful proof-of-principle experiments shortly before graduating. The project was picked up again in 2023 by Dr. Theresa Gozzo, Christopher Weir, and me. Early experiments were focused on understanding the source, its limits, and replicating the proof-of-principle experiments We made minor modifications to the source for improved safety and ease of use.

The ptESI source allows us to rapidly scan across a broad range of temperatures while continuously acquire mass spectra. The first iteration of the source was used to control the source temperature during cation-to-anion proton transfer reaction (CAPTR) experiments using cytochrome c.[44] Like many other designs, a Peltier thermoelectric chip is incorporated; controlled by a digital temperature controller, it heats and cools a small copper block. This

copper block is placed on top of the Peltier and has an embedded thermistor that measures the block temperature and a hole drilled through it for a capillary tip. The temperature controller adjusts the current supplied to the Peltier based on the reading from the thermistor. Thermal connections are made using thermal paste. A 3D-printed clamp maintains even pressure on the Peltier and helps hold everything in place. The nESI capillary is positioned inside the copper block with the tip pointing towards the instrument inlet. The source is mounted on an xyz stage to enable the tip position to be finely tuned. A platinum wire is inserted into the wide end of the capillary to apply the electrospray voltage. Only 3 – 5 µL of solution is required for a single experiment.

The ptESI source is capable of scanning temperatures between 5 – 97 ˚C at rates of up to 120 ˚C·min^{-1}. The desired start, end, and optional midpoint incubation temperatures, scan rates between temperature steps, incubation times, number of cycles, and desired waveform are set using a custom Python program. Characterization experiments were performed by measuring the temperature of an ammonium acetate solution using a thermocouple inserted into a pulled capillary tip. The temperature inside the capillary was monitored using a thermocouple data acquisition device and compared to the temperature recorded by the embedded thermistor. The two measured temperatures are in close agreement with each other and the programmed temperature throughout repeated thermal cycles. From this, the block temperature measured by the thermistor can be used as a proxy for the temperature of the solution inside the capillary. ptESI experiments can be performed very rapidly. At a scan rate of 30 ˚C·min^{-1}, scanning from 10 – 90 ˚C takes ~2.5 min, during which mass spectra are continuously recorded. With an MS scan rate of 60 scans·min^{-1}, 150+ mass spectra are acquired during the temperature ramp. Although many previous tcESI studies have determined the melting curves for various model

proteins, they have neglected to thoroughly investigate the cooling phase during which the protein may refold. The ptESI source is easily programmed for thermal cycles, in which the temperature is scanned from low to high, and back to the initial low temperature at a set scan rate. Both the heating and cooling phases are controlled while acquiring mass spectra. At a scan rate of 15 ˚C.min^{-1}, scanning from 10 – 90 – 10 ˚C takes just over 10 min and 600+ mass spectra are recorded. A sample can be cycled any number of times, the number of cycles is set in the program. The rapidity of scanning with ptESI may help avoid aggregation, as shorter periods of time are spent at elevated temperatures. Though ptESI may not be as fast as the laser heated source, it has active cooling capabilities and results in shorter and more data-dense experiments than tcESI sources. In this work, ptESI is used to investigate both the unfolding *and* refolding transitions of the model proteins ubiquitin and lysozyme through thermal cycling experiments at multiple scan rates.

References

(1) Anfinsen, C. B. Principles That Govern the Folding of Protein Chains. *Science* **1973**, *181* (4096), 223–230.

(2) Hingorani, K. S.; Gierasch, L. M. Comparing Protein Folding In Vitro and In Vivo: Foldability Meets the Fitness Challenge. *Curr. Opin. Struct. Biol.* **2014**, *0*, 81–90. https://doi.org/10.1016/j.sbi.2013.11.007.

(3) Creighton, T. E. Protein Folding. *Biochem. J.* **1990**, *270* (1), 1–16.

(4) Privalov, P. L.; Khechinashvili, N. N. A Thermodynamic Approach to the Problem of Stabilization of Globular Protein Structure: A Calorimetric Study. *J. Mol. Biol.* **1974**, *86* (3), 665–684. https://doi.org/10.1016/0022-2836(74)90188-0.

(5) Privalov, P. L.; Dragan, A. I. Microcalorimetry of Biological Macromolecules. *Biophys. Chem.* **2007**, *126* (1–3), 16–24. https://doi.org/10.1016/j.bpc.2006.05.004.

(6) Chaires, J. B. Calorimetry and Thermodynamics in Drug Design. *Annu. Rev. Biophys.* **2008**, *37* (1), 135–151. https://doi.org/10.1146/annurev.biophys.36.040306.132812.

(7) Jacobson, A. L.; Braun, H. Differential Scanning Calorimetry of the Thermal Denaturation of Lactate Dehydrogenase. *Biochim. Biophys. Acta BBA - Protein Struct.* **1977**, *493* (1), 142–153. https://doi.org/10.1016/0005-2795(77)90267-7.

(8) Vagenende, V.; Yap, M. G. S.; Trout, B. L. Mechanisms of Protein Stabilization and Prevention of Protein Aggregation by Glycerol. *Biochemistry* **2009**, *48* (46), 11084–11096. https://doi.org/10.1021/bi900649t.

(9) Gaisford, S. Fast-Scan Differential Scanning Calorimetry. *Eur. Pharm. Rev.*

(10) Mukhametzyanov, T. A.; Sedov, I. A.; Solomonov, B. N.; Schick, C. Fast Scanning Calorimetry of Lysozyme Unfolding at Scanning Rates from 5 K/Min to 500,000 K/Min.

Biochim. Biophys. Acta BBA - Gen. Subj. **2018**, *1862* (9), 2024–2030. https://doi.org/10.1016/j.bbagen.2018.06.019.

(11) Garbett, N. C.; Chaires, J. B. Thermodynamic Studies for Drug Design and Screening. *Expert Opin. Drug Discov.* **2012**, *7* (4), 299–314. https://doi.org/10.1517/17460441.2012.666235.

(12) Lang, B. E.; Cole, K. D. Differential Scanning Calorimetry and Fluorimetry Measurements of Monoclonal Antibodies and Reference Proteins: Effect of Scanning Rate and Dye Selection. *Biotechnol. Prog.* **2017**, *33* (3), 677–686. https://doi.org/10.1002/btpr.2464.

(13) Niesen, F. H.; Berglund, H.; Vedadi, M. The Use of Differential Scanning Fluorimetry to Detect Ligand Interactions That Promote Protein Stability. *Nat. Protoc.* **2007**, *2* (9), 2212–2221. https://doi.org/10.1038/nprot.2007.321.

(14) He, F.; Hogan, S.; Latypov, R. F.; Narhi, L. O.; Razinkov, V. I. High Throughput Thermostability Screening of Monoclonal Antibody Formulations. *J. Pharm. Sci.* **2010**, *99* (4), 1707–1720. https://doi.org/10.1002/jps.21955.

(15) Greenfield, N. J. Using Circular Dichroism Collected as a Function of Temperature to Determine the Thermodynamics of Protein Unfolding and Binding Interactions. *Nat. Protoc.* **2006**, *1* (6), 2527–2535. https://doi.org/10.1038/nprot.2006.204.

(16) Sreerama, N.; Venyaminov, S. Yu.; Woody, R. W. Estimation of Protein Secondary Structure from Circular Dichroism Spectra: Inclusion of Denatured Proteins with Native Proteins in the Analysis. *Anal. Biochem.* **2000**, *287* (2), 243–251. https://doi.org/10.1006/abio.2000.4879.

(17) Kelly, S. M.; Price, N. C. The Application of Circular Dichroism to Studies of Protein Folding and Unfolding. *Biochim. Biophys. Acta BBA - Protein Struct. Mol. Enzymol.* **1997**, *1338* (2), 161–185. https://doi.org/10.1016/S0167-4838(96)00190-2.

(18) Davoodi, J.; Wakarchuk, W. W.; Surewicz, W. K.; Carey, P. R. Scan-rate dependence in protein calorimetry: The reversible transitions of Bacillus circulans xylanase and a disulfide-bridge mutant. *Protein Sci.* **1998**, *7* (7), 1538–1544. https://doi.org/10.1002/pro.5560070707.

(19) Lepock, J. R.; Ritchie, K. P.; Kolios, M. C.; Rodahl, A. M.; Heinz, K. A.; Kruuv, J. Influence of Transition Rates and Scan Rate on Kinetic Simulations of Differential Scanning Calorimetry Profiles of Reversible and Irreversible Protein Denaturation. *Biochemistry* **1992**, *31* (50), 12706–12712. https://doi.org/10.1021/bi00165a023.

(20) Damgaard, R. B. The Ubiquitin System: From Cell Signalling to Disease Biology and New Therapeutic Opportunities. *Cell Death Differ.* **2021**, *28* (2), 423–426. https://doi.org/10.1038/s41418-020-00703-w.

(21) Jackson, S. E. Ubiquitin: A Small Protein Folding Paradigm. *Org. Biomol. Chem.* **2006**, *4* (10), 1845–1853. https://doi.org/10.1039/B600829C.

(22) Wintrode, P. L.; Makhatadze, G. I.; Privalov, P. L. Thermodynamics of Ubiquitin Unfolding. *Proteins* **1994**, *18* (3), 246–253. https://doi.org/10.1002/prot.340180305.

(23) Kugimiya, M.; Bigelow, C. C. The Denatured States of Lysozyme. *Can. J. Biochem.* **1973**, *51* (5), 581–585. https://doi.org/10.1139/o73-072.

(24) Lee, J. W.; Kim, H. I. Investigating Acid-Induced Structural Transitions of Lysozyme in an Electrospray Ionization Source. *The Analyst* **2015**, *140* (2), 661–669. https://doi.org/10.1039/C4AN01794C.

(25) Sasahara, K.; Demura, M.; Nitta, K. Equilibrium and Kinetic Folding of Hen Egg-White Lysozyme under Acidic Conditions. *Proteins Struct. Funct. Bioinforma.* **2002**, *49* (4), 472–482. https://doi.org/10.1002/prot.10215.

(26) Leney, A. C.; Heck, A. J. R. Native Mass Spectrometry: What Is in the Name? *J. Am. Soc. Mass Spectrom.* **2017**, *28* (1), 5–13. https://doi.org/10.1007/s13361-016-1545-3.

(27) Wang, G.; Abzalimov, R. R.; Kaltashov, I. A. Direct Monitoring of Heat-Stressed Biopolymers with Temperature-Controlled Electrospray Ionization Mass Spectrometry. *Anal. Chem.* **2011**, *83* (8), 2870–2876. https://doi.org/10.1021/ac200441a.

(28) Mirza, U. A.; Cohen, S. L.; Chait, B. T. Heat-Induced Conformational Changes in Proteins Studied by Electrospray Ionization Mass Spectrometry. *Anal. Chem.* **1993**, *65* (1), 1–6. https://doi.org/10.1021/ac00049a003.

(29) Benesch, J. L. P.; Sobott, F.; Robinson, C. V. Thermal Dissociation of Multimeric Protein Complexes by Using Nanoelectrospray Mass Spectrometry. *Anal. Chem.* **2003**, *75* (10), 2208–2214. https://doi.org/10.1021/ac034132x.

(30) Geels, R. B. J.; Calmat, S.; Heck, A. J. R.; van der Vies, S. M.; Heeren, R. M. A. Thermal Activation of the Co-Chaperonins GroES and Gp31 Probed by Mass Spectrometry. *Rapid Commun. Mass Spectrom.* **2008**, *22* (22), 3633–3641. https://doi.org/10.1002/rcm.3782.

(31) Cong, X.; Liu, Y.; Liu, W.; Liang, X.; Russell, D. H.; Laganowsky, A. Determining Membrane Protein–Lipid Binding Thermodynamics Using Native Mass Spectrometry. *J. Am. Chem. Soc.* **2016**, *138* (13), 4346–4349. https://doi.org/10.1021/jacs.6b01771.

(32) Lippens, J. L.; Mangrum, J. B.; McIntyre, W.; Redick, B.; Fabris, D. A Simple Heated-Capillary Modification Improves the Analysis of Non-Covalent Complexes by Z-Spray

Electrospray Ionization. *Rapid Commun. Mass Spectrom.* **2016**, *30* (6), 773–783. https://doi.org/10.1002/rcm.7490.

(33) El-Baba, T. J.; Woodall, D. W.; Raab, S. A.; Fuller, D. R.; Laganowsky, A.; Russell, D. H.; Clemmer, D. E. Melting Proteins: Evidence for Multiple Stable Structures upon Thermal Denaturation of Native Ubiquitin from Ion Mobility Spectrometry-Mass Spectrometry Measurements. *J. Am. Chem. Soc.* **2017**, *139* (18), 6306–6309. https://doi.org/10.1021/jacs.7b02774.

(34) El-Baba, T. J.; Clemmer, D. E. Solution Thermochemistry of Concanavalin A Tetramer Conformers Measured by Variable-Temperature ESI-IMS-MS. *Int. J. Mass Spectrom.* **2019**, *443*, 93–100. https://doi.org/10.1016/j.ijms.2019.06.004.

(35) McCabe, J. W.; Shirzadeh, M.; Walker, T. E.; Lin, C.-W.; Jones, B. J.; Wysocki, V. H.; Barondeau, D. P.; Clemmer, D. E.; Laganowsky, A.; Russell, D. H. Variable-Temperature Electrospray Ionization for Temperature-Dependent Folding/Refolding Reactions of Proteins and Ligand Binding. *Anal. Chem.* **2021**, *93* (18), 6924–6931. https://doi.org/10.1021/acs.analchem.1c00870.

(36) Hommersom, B.; Porta, T.; Heeren, R. M. A. Ion Mobility Spectrometry Reveals Intermediate States in Temperature-Resolved DNA Unfolding. *Int. J. Mass Spectrom.* **2017**, *419*, 52–55. https://doi.org/10.1016/j.ijms.2017.03.008.

(37) Marchand, A.; Rosu, F.; Zenobi, R.; Gabelica, V. Thermal Denaturation of DNA G-Quadruplexes and Their Complexes with Ligands: Thermodynamic Analysis of the Multiple States Revealed by Mass Spectrometry. *J. Am. Chem. Soc.* **2018**, *140* (39), 12553–12565. https://doi.org/10.1021/jacs.8b07302.

(38) Pruška, A.; Marchand, A.; Zenobi, R. Novel Insight into Proximal DNA Domain Interactions from Temperature-Controlled Electrospray Ionization Mass Spectrometry. *Angew. Chem. Int. Ed.* **2021**, *60* (28), 15390–15398. https://doi.org/10.1002/anie.202016757.

(39) Liu, J.; Wang, Y.; Wang, X.; Qin, W.; Li, G. Measuring Protein Unfolding Thermodynamic Stability in One Minute with Digital Temperature Control-Equipped nanoESI-Mass Spectrometry. *Int. J. Mass Spectrom.* **2023**, *494*, 117151. https://doi.org/10.1016/j.ijms.2023.117151.

(40) Daneshfar, R.; Kitova, E. N.; Klassen, J. S. Determination of Protein−Ligand Association Thermochemistry Using Variable-Temperature Nanoelectrospray Mass Spectrometry. *J. Am. Chem. Soc.* **2004**, *126* (15), 4786–4787. https://doi.org/10.1021/ja0316972.

(41) Raab, S. A.; El-Baba, T. J.; Woodall, D. W.; Liu, W.; Liu, Y.; Baird, Z.; Hales, D. A.; Laganowsky, A.; Russell, D. H.; Clemmer, D. E. Evidence for Many Unique Solution Structures for Chymotrypsin Inhibitor 2: A Thermodynamic Perspective Derived from vT-ESI-IMS-MS Measurements. *J. Am. Chem. Soc.* **2020**, *142* (41), 17372–17383. https://doi.org/10.1021/jacs.0c05365.

(42) Woodall, D. W.; Henderson, L. W.; Raab, S. A.; Honma, K.; Clemmer, D. E. Understanding the Thermal Denaturation of Myoglobin with IMS-MS: Evidence for Multiple Stable Structures and Trapped Pre-Equilibrium States. *J. Am. Soc. Mass Spectrom.* **2021**, *32* (1), 64–72. https://doi.org/10.1021/jasms.0c00075.

(43) Jordan, J. S.; Williams, E. R. Laser Heating Nanoelectrospray Emitters for Fast Protein Melting Measurements with Mass Spectrometry. *Anal. Chem.* **2022**, *94* (48), 16894–16900. https://doi.org/10.1021/acs.analchem.2c04204.

(44) Laszlo, K. J.; Buckner, J. H.; Munger, E. B.; Bush, M. F. Native-Like and Denatured Cytochrome *c* Ions Yield Cation-to-Anion Proton Transfer Reaction Products with Similar Collision Cross-Sections. *J. Am. Soc. Mass Spectrom.* **2017**, *28* (7), 1382–1391. https://doi.org/10.1007/s13361-017-1620-4.

(45) Leney, A. C.; Heck, A. J. R. Native Mass Spectrometry: What Is in the Name? *J. Am. Soc. Mass Spectrom.* **2017**, *28* (1), 5–13. https://doi.org/10.1007/s13361-016-1545-3.

(46) El-Baba, T. J.; Raab, S. A.; Buckley, R. P.; Brown, C. J.; Lutomski, C. A.; Henderson, L. W.; Woodall, D. W.; Shen, J.; Trinidad, J. C.; Niu, H.; Jarrold, M. F.; Russell, D. H.; Laganowsky, A.; Clemmer, D. E. Thermal Analysis of a Mixture of Ribosomal Proteins by vT-ESI-MS: Toward a Parallel Approach for Characterizing the Stabilitome. *Anal. Chem.* **2021**, *93* (24), 8484–8492. https://doi.org/10.1021/acs.analchem.1c00772.

(47) Giles, K.; Ujma, J.; Wildgoose, J.; Pringle, S.; Richardson, K.; Langridge, D.; Green, M. A Cyclic Ion Mobility-Mass Spectrometry System. *Anal. Chem.* **2019**, *91* (13), 8564–8573. https://doi.org/10.1021/acs.analchem.9b01838.

(48) Aune, K. C.; Salahuddin, A.; Zarlengo, M. H.; Tanford, C. Evidence for Residual Structure in Acid- and Heat-Denatured Proteins. *J. Biol. Chem.* **1967**, *242* (19), 4486–4489. https://doi.org/10.1016/S0021-9258(18)99563-3.

(49) Haezebrouck, P.; Joniau, M.; Van Dael, H.; Hooke, S. D.; Woodruff, N. D.; Dobson, C. M. An Equilibrium Partially Folded State of Human Lysozyme at Low pH. *J. Mol. Biol.* **1995**, *246* (3), 382–387. https://doi.org/10.1006/jmbi.1994.0093.

(50) Tanford, C.; Aune, K. C.; Ikai, A. Kinetics of Unfolding and Refolding of Proteins: III. Results for Lysozyme. *J. Mol. Biol.* **1973**, *73* (2), 185–197. https://doi.org/10.1016/0022-2836(73)90322-7.

(51) Kuwajima, K.; Hiraoka, Y.; Ikeguchi, M.; Sugai, S. Comparison of the Transient Folding Intermediates in Lysozyme and .Alpha.-Lactalbumin. *Biochemistry* **1985**, *24* (4), 874–881. https://doi.org/10.1021/bi00325a010.

(52) Kiefhaber, T. Kinetic Traps in Lysozyme Folding. *Proc. Natl. Acad. Sci.* **1995**, *92* (20), 9029–9033. https://doi.org/10.1073/pnas.92.20.9029.

(53) Kotov, V.; Mlynek, G.; Vesper, O.; Pletzer, M.; Wald, J.; Teixeira-Duarte, C. M.; Celia, H.; Garcia-Alai, M.; Nussberger, S.; Buchanan, S. K.; Morais-Cabral, J. H.; Loew, C.; Djinovic-Carugo, K.; Marlovits, T. C. In-Depth Interrogation of Protein Thermal Unfolding Data with MoltenProt. *Protein Sci.* **2021**, *30* (1), 201–217. https://doi.org/10.1002/pro.3986.

(54) Van Berkel, G. J.; Asano, K. G.; Schnier, P. D. Electrochemical Processes in a Wire-in-a-Capillary Bulk-Loaded, Nano-Electrospray Emitter. *J. Am. Soc. Mass Spectrom.* **2001**, *12* (7), 853–862. https://doi.org/10.1016/S1044-0305(01)00264-1.

(55) Gadzuk-Shea, M. M.; Hubbard, E. E.; Gozzo, T. A.; Bush, M. F. Sample pH Can Drift during Native Mass Spectrometry Experiments: Results from Ratiometric Fluorescence Imaging. *J. Am. Soc. Mass Spectrom.* **2023**, *34* (8), 1675–1684. https://doi.org/10.1021/jasms.3c00147.

(56) Savitzky, Abraham.; Golay, M. J. E. Smoothing and Differentiation of Data by Simplified Least Squares Procedures. *Anal. Chem.* **1964**, *36* (8), 1627–1639. https://doi.org/10.1021/ac60214a047.

(57) Creighton, T. E. The Energetic Ups and Downs of Protein Folding. *Nat. Struct. Biol.* **1994**, *1* (3), 135–138. https://doi.org/10.1038/nsb0394-135.

(58) Gozzo, T. A.; Weir, C. J.; Constabel, M. A.; Bush, M. F. Selecting Reducing Agents for Native Mass Spectrometry. ChemRxiv February 1, 2024. https://doi.org/10.26434/chemrxiv-2024-2nmh4-v2.

(59) Duckworth, H. W.; Nguyen, N. T.; Gao, Y.; Donald, L. J.; Maurus, R.; Ayed, A.; Bruneau, B.; Brayer, G. D. Enzyme–Substrate Complexes of Allosteric Citrate Synthase: Evidence for a Novel Intermediate in Substrate Binding. *Biochim. Biophys. Acta BBA - Proteins Proteomics* **2013**, *1834* (12), 2546–2553. https://doi.org/10.1016/j.bbapap.2013.07.019.

(60) Bai, J.-H.; Wang, H.-J.; Liu, D.-S.; Zhou, H.-M. Kinetics of Thermal Inactivation of Lactate Dehydrogenase from Rabbit Muscle. *J. Protein Chem. 16* (8).

CHAPTER II

Evaluating the Reversible Unfolding of Ubiquitin and Lysozyme at Low pH Using Programmed Temperature ESI (ptESI)

Introduction

Temperature is a popular method to manipulate protein structure to probe protein folding, as it is a "universal factor of influence with a fundamental physical meaning."[4] Protein folding or misfolding is being increasingly linked to disease, yet the process through which it occurs is not yet fully understood. Commonly used thermal techniques such as differential scanning calorimetry (DSC), differential scanning fluorimetry (DSF), and circular dichroism (CD) have been used to study the folding kinetics, conformational states, and stabilities of proteins. DSC provides precise and direct measurements of molar heat capacity of unfolding events, melting temperature, and other thermodynamic parameters.[5,6] It is limited by slow scan rates and low throughput experiments and also requires large sample volumes, which can be challenging to obtain for many analytes of interest. Scan rate dependence has been well documented in DSC. Previously, it was only thought to arise during irreversible transitions, but the melting temperature shifting to higher temperatures with increasing scan rate was observed for the reversible thermal denaturation of xylanase.[18] DSC is very good for obtaining thermodynamic values but offers no additional structural or conformational information.

In comparison, DSF provides a measurement of melting temperature, but also some conformational information through fluorescence as this technique uses dyes that fluoresce in non-polar environments, such as hydrophobic pockets in protein structure.[11] As the temperature increases, the protein unfolds and the dye interacts with the exposed hydrophobic sites resulting in increased fluorescence intensity. DSF experiments are often performed using real-time PCR

instruments, which are widely available, require smaller sample volumes, and are compatible with multiplexing through multi-well plates.[11] However, not all protein-dye combinations will result in a detectable melting transition.[12] A large excess of dye is added, which can perturb the system and result in errors in measurement.[11] Both DSC and DSF are calorimetric methods that can be used to monitor changes in melting temperature to assess changes in stability, which is useful for binding assays.

CD is an optical method that is sensitive to structure and allows for a more direct measurement of protein secondary structure, as α-helices and ß-sheets have characteristic spectra at specific wavelengths of light[15] and far-UV CD is sensitive to changes in protein backbone conformation.[16] Most CD instruments are not capable of scanning temperature, thus spectra must be acquired at points over a range of temperatures, resulting in time-consuming experiments.[15] Thermodynamic parameters can be estimated only if there is a single unfolding event and the unfolding is reversible.[15] Overall, these common techniques provide limited information and work best when simple unfolding transitions are occurring.

Nanoelectrospray ionization-mass spectrometry (nESI-MS) provides detailed structural information about biomolecules in physiologically relevant solution conditions. Changing the temperature experienced by sample in the nESI capillary changes the conformation of the protein in solution, which is at least partially maintained through transfer into the gas phase.[45] This technique has been developing rapidly and encompasses sources called variable-temperature ESI (vt-ESI),[33,34,41,35,46] digital temperature control-ESI (DTC-ESI)[39], laser heating ESI (LH-ESI)[43], and temperature-controlled-ESI (TC-ESI).[37,38] Many of these sources use Peltier thermoelectric devices to control the temperature of a metal block.

Here, we will describe our programmed temperature-ESI (ptESI) source design to control solution temperature of a nESI capillary during thermal cycling experiments. We will apply this source to characterize the unfolding and refolding with heating and cooling of ubiquitin and lysozyme are measured at different scan rates through changes in average charge state. Determination of midpoint temperatures (T_m) and characterization of transitions can be done rapidly.

Materials and Methods

Sample Preparation

Lysozyme from hen egg white (62970, Sigma-Aldrich, St. Louis, MO) was dissolved in MilliQ ultra-pure water (EMD Millipore, Burlington, MA) and adjusted to pH 2 using glacial acetic acid (A-35, Fisher Scientific, Rockwood, TN) to a final protein concentration of 3 μM. Recombinant human ubiquitin (U-100H, R&D Systems, Minneapolis, MN) was dissolved in aqueous acetic acid at pH 2.15 to a final protein concentration of 4 μM. For the multiplex experiment, ubiquitin and lysozyme were dissolved in aqueous acetic acid at pH 2.15 at 2 μM, for a total protein concentration of 4 μM. Sample pH was measured using a micro pH probe (ThermoFisher Scientific, Waltham, MA).

ptESI and Mass Spectrometry Settings

Our ptESI source (Fig. S1) scans between starting, high, and ending temperatures programmed by the experimenter at scan rates. A full description of the source and its capabilities are included in the Supplemental Information. Source characterization experiments have shown a close agreement between the temperature inside the capillary, block temperature, and programmed temperature (Fig. S2).

For tcESI experiments, the program starts at 10 °C and ends at 90 °C, with 4-minute incubation steps at 5 °C increments. The temperature is increased at a rate of 5 °C.min^{-1} between incubation periods. For ptESI experiments, the temperature scans from 10 – 90 °C at 9, 15, or 30 °C·min^{-1}. For thermal cycling experiments, the temperature scans from 10 – 90 – 10 °C at 9, 15, or 30 °C·min^{-1} for the specified number of cycles.

Five µL of sample was loaded into a borosilicate glass capillaries pulled to a 1-3 µm tip (Sutter Instruments Model P-97), then inserted into the ptESI source held at 10 °C. Electrical contact with the solution was made using a platinum wire electrode inserted into the wide end of the capillary. Electrospray was established by applying 0.4 to 0.7 kV of potential to the electrode. Mass spectra were acquired using a SELECT SERIES Cyclic IMS instrument[47] at a rate of 1 scan·second^{-1}. Mass spectra were calibrated using cesium iodide. Mass spectral data was worked up in a Jupyter notebook using custom Python tools developed in-house that use the Waters SDK to interact directly with raw data files. The extracted ion chromatograms (Fig. S3) for each charge state are generated using specified mass ranges and the average charge state is calculated using the intensity of the extracted ion chromatogram as a weight for each charge state. The temperature readings from the embedded thermistor in the ptESI source are used to link experiment time and block temperature. The average charge state and temperature are plotted and sigmoidal curve fitting is done using Equation S1.

Results and Discussion

Using ptESI to Study Protein Folding

In this work we will use tcESI to refer to approaches or methods that take measurements at discrete, pre-determined temperatures and allow time – typically several minutes – after

changing the temperature before acquiring mass spectral data. Figure 1A shows the temperature program for a tcESI experiment adapted for ptESI. The program replicates typical tcESI experiments with several minute equilibration and acquisition times at each temperature step, resulting in an experiment duration of ~90 minutes. The average charge state of ubiquitin is plotted over time (Fig. 1B). The temperature steps are visible in the average charge state plot. The insets indicate the mass spectra acquired at the lowest and highest temperatures.

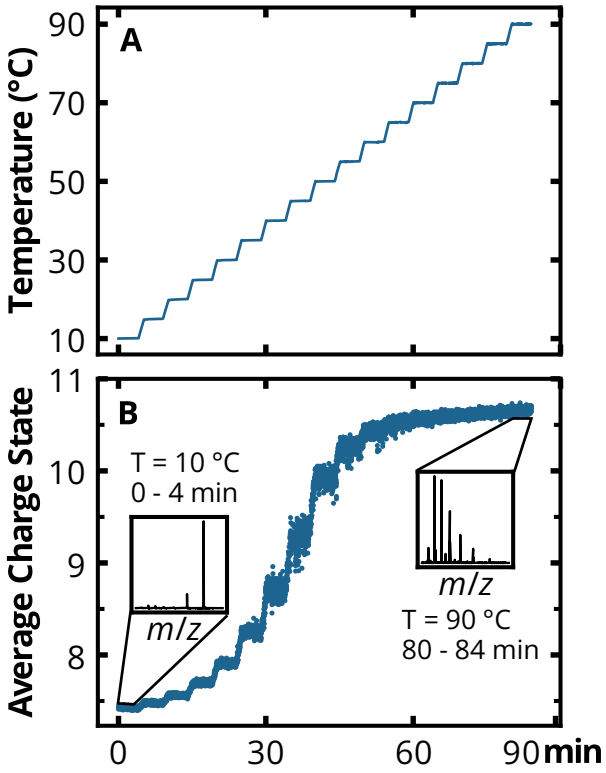

Figure 1. TC-ESI style program and results for the unfolding of ubiquitin at pH 2.15. (A) tcESI style stepped temperature program scanning from 10 – 90 °C, with 4 minute incubation periods every 5 °C. This program has a duration of 84 minutes. (B) Unfolding curve obtained using the program in A. The changes in temperature are reflected in the average charge state. The insets show the mass spectra acquired at the lowest and highest temperature incubations, along with the time.

The tcESI-style program (Fig. 1A) incubates for 4 minutes to reflect the longer duration of time spent at each temperature step in a typical tcESI experiment: 1 – 2 minutes of equilibration before 1 – 2 minutes of mass spectral acquisition. Average charge state ($\bar{z}$) is an established measure of protein unfolding in native MS, as the number of protons that a protein can carry depends on the extent of unfolding. It is a weighted average based on the intensity of the charge state peaks in the mass spectrum. Each data point in Figure 1B is the average charge state calculated from a single mass spectral scan of ubiquitin acquired at the corresponding temperature point. Representative mass spectra for the highest and lowest temperatures are shown in the insets; the charge state distribution shifts dramatically from low to high temperature. The sigmoidal transition can be curve fit and the midpoint temperature of unfolding (T_m) determined by the inflection point of the fit.[29] The tcESI-style experiments resulted in a T_m of 42.2 ± 0.2 °C, which is consistent with all other T_m values determined in this study. The T_m values obtained do not agree with results from a previous DSC study[22]; however, in that study, the transition was irreversible. The reversibility of the transition studied using ptESI is discussed later.

Ubiquitin is a small, monomeric, highly conserved protein in eukaryotes with 76 residues. It is commonly used as a model system for protein studies due to its abundance, stability, and highly structured native conformation.[21] However, because ubiquitin is so stable, the solution must be at low pH to destabilize the native structure in order to obtain an unfolding transition between 0 – 100 °C. In this tcESI type experiment, the need for equilibration and acquisition time at each temperature results in longer experiment times, thus the selection of

temperature points, the increments in between, equilibration and acquisition times must balance good coverage across the melting curve and reasonable experiment times.

Varying the temperature scan rate reveals differing behaviour for different proteins. The temperature program is shown by the measured block temperature (Fig. 2A) during scans of ubiquitin at rates of 9, 15, and 30 °C·min^{-1}. Figure 2B shows the corresponding unfolding curves of ubiquitin. The three curves for the three different rates are overlaid and give a T_m of 47.5 ± 2.4 °C. In contrast, the unfolding curves of lysozyme (Fig. 2C) shows the curves shift to lower temperatures with increasing scan rates. The three curves at 9, 15, and 30 °C·min^{-1} give T_m of 56.2, 60.3, and 69.2 °C, respectively.

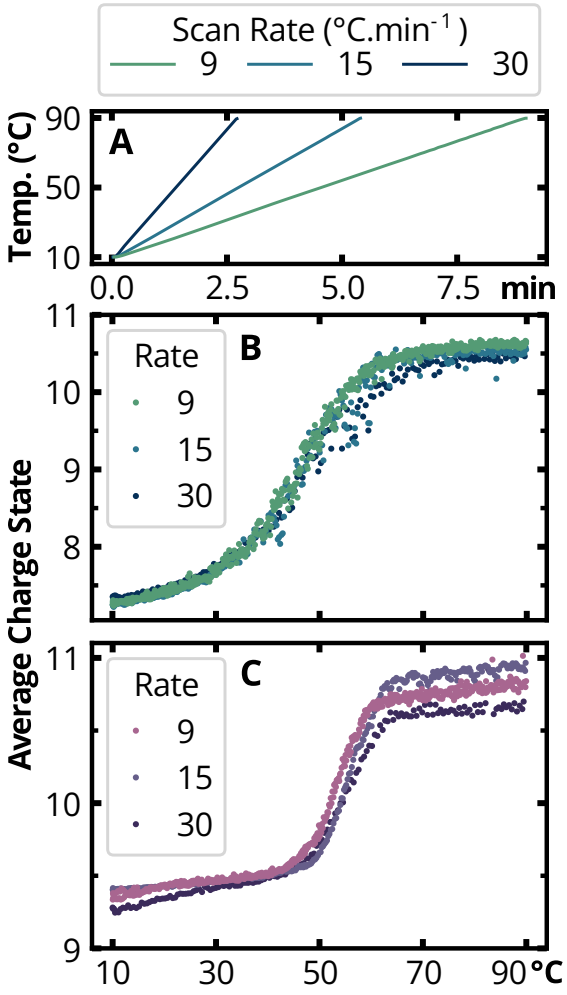

Figure 2. Unfolding curves for ubiquitin and lysozyme acquired using ptESI. A) The temperature program is reflected in the measured block temperature for the three different scans of ubiquitin at the three scan rates investigated. The lysozyme data were acquired using the same temperature programs and are indistinguishable from the block temperatures shown. B) Unfolding curves of ubiquitin at 9, 15, and 30 °C.min^{-1}. All three curves overlap well. C) Unfolding curves of lysozyme at 9, 15, and 30 °C.min^{-1}. The transition and thus T_m values shift to higher temperatures with increasing scan rate.

Our ptESI source allows for rapid acquisition of thermal cycling data, in which mass spectra are acquired continuously. Compared to the tcESI experiment in Fig. 1, the same data is acquired in under 5 minutes using ptESI. The curve in Figure 2B resembles previously those reported in tcESI studies of ubiquitin, but the T_m values differ as those studies used a higher pH.[33,35] Small proteins like ubiquitin and lysozyme are expected to fold quickly, on the order of micro- to milliseconds.[2] From this, we assume that the protein is in equilibrium throughout the measurement, as the rate of folding is faster than the scan rate. Lysozyme is another small, monomeric protein, with 129 residues and 4 disulfide bonds. Like ubiquitin, it is a common model protein used in folding studies, as is known to retain its folded structure and remain stable at low pH.[48,49] Lysozyme also has the expected sigmoidal unfolding transition (Fig. 2C), but it shifts to lower temperatures with increasing scan rate. The apparent scan rate dependence of lysozyme unfolding indicates that it may not be in equilibrium during the unfolding transition and there is a kinetic component. While there have been previous studies of acidified lysozyme discussing pH guanidinium chloride dependence,[50–52] few have indicated a scan-rate dependence.[25] Scan rate dependence will be discussed more in depth further on. It is important to

note that the slope of the sigmoid differs between the ubiquitin and lysozyme curves. A steeper slope corresponds to unfolding beginning later, and the folded protein state being more resistant to increasing temperatures.[53] The folding transition of ubiquitin is highly sensitive to pH, and very small changes in pH result in large shifts of the curves (Fig. S4). Because the slope of the transition is less steep, it is more difficult to capture the full transition between 10 – 90 °C. The ptESI source is capable of heating and cooling between 5 – 97 °C, but it is currently optimized to operate between 10 – 90 °C. The continuous acquisition of mass spectra results in data dense experiments with many more points across the unfolding transition compared to tcESI experiments. The ease of determining T_m using ptESI make a potential candidate for use in thermal stability and binding assay as part of drug development programs.

Using ptESI To Study Protein Refolding

Figure 3A shows the block temperature for a single cycle program with a gradient of ±30 °C·min^{-1}. Here, a thermal cycle is defined as scanning from a low temperature to a high temperature, and back to the starting low temperature at a set scan rate. Figures 3B and 3C show average charge state plots for single thermal cycles of ubiquitin and lysozyme, respectively.

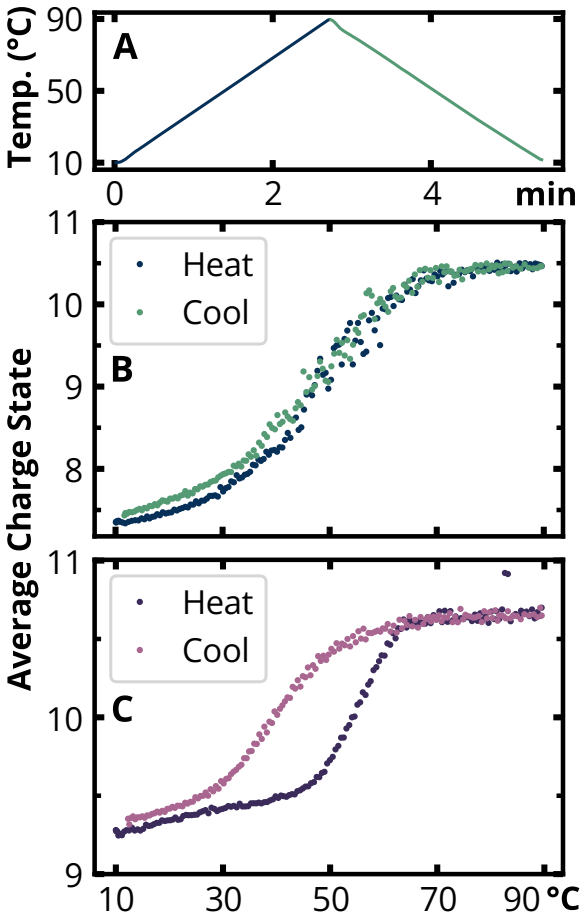

Figure 3. Single thermal cycles of ubiquitin and lysozyme at 30 °C·min^{-1}. A) The block temperature for a single thermal cycle of ubiquitin, reflecting the programmed temperature. The block temperatures for lysozyme are indistinguishable. B) The average charge state over a single thermal cycle of ubiquitin. The data points from the heating phase are in dark blue and those from the cooling phase are in light blue-green. The two curves overlap. C) The average charge state over a single thermal cycle of lysozyme. The data points from the heating phase are in dark purple and those from the cooling phase are in pink. The two curves do not overlap during the transition.

A strength of the ptESI source is the ease in which thermal cycling experiments can be performed. In a thermal cycle, both the unfolding and refolding of the protein are captured, unlike in the heating-only curve in Figure 1. The importance of studying refolding is difficult to overstate, as protein folding is critical to forming functional proteins as part of normal physiology. The melting or unfolding curve is acquired during heating and the refolding curve is acquired during cooling. For a single thermal cycle of ubiquitin (Fig. 3B), the refolding curve overlaps with the unfolding curve. The T_m values for the heating and cooling phases are very similar, 47.0 and 45.9 °C, respectively. The average charge state returns to the initial value, indicating complete refolding and a reversible transition. Previous work has demonstrated the reversible unfolding of ubiquitin at low pH by first incubating at 90 °C before cooling the sample and analyzing at 26 °C.[33] The results were found to be indistinguishable from samples that had not been heated, but the sample was not monitored during cooling. The results shown in Fig. 3B demonstrate the reversibility while monitoring the refolding transition. With ptESI, evaluating the reversibility of the unfolding transition is easy. The average charge state returning to near the initial value at the end of a cycle indicates reversible unfolding. Compared to DSC, this does not require a second scan and can be done as part of the same acquisition. The overlap of the unfolding and refolding curves of ubiquitin suggests that the two transitions are very similar in cooperativity and likely occur through similar processes, further emphasizing the reversibility of unfolding.

For a single thermal cycle of lysozyme (Fig. 3C), the average charge state also returns to the initial value, but there is a significant difference between the unfolding and refolding curves, as they do not overlap during the transition. The T_m values for the heating and cooling phases are quite different, 54.1 and 39.4 °C, respectively. The change in T_m between the unfolding and

refolding curves (ΔT_m) suggests that the unfolding and refolding processes are more different. Protein refolding is usually a more complex compared to unfolding, as the unfolded state is conformationally more heterogeneous.[3] A previous tcESI study noted that the high charge states of lysozyme in the high temperature mass spectra appear similar to spectra in which disulfide scrambling has occurred.[27] It is unlikely that disulfide scrambling is occurring, as the protein would be trapped in unfolded conformations with high average charge state upon cooling and the average charge state returns its low initial value, indicating the protein is refolding. This is discussed further in the Supplementary Information. Other studies have shown that at elevated temperatures, lysozyme retains its disulfide bonds.[23,48] It has been suggested that isomers of the unfolded polypeptide chain could get tangled in loops formed by the maintained disulfide bonds, resulting in slow refolding pathways.[52] Kiefhaber also stated that if there is a partially folded state refolding slowly with a sequential folding mechanism, there would be a "lag phase […] in the formation of native molecules",[52] which arises in these ptESI data as ΔT_m.

Repeated Thermal Cycling

The block temperature for a thermal cycling program of ubiquitin is shown in Figure 4A. At a rate of ±30 °C·min^{-1}, three thermal cycles take in ~15 minutes. Plotting the average charge state versus time (Fig. 4B) shows the average charge state changing with thermal cycling. Plotting the average charge state versus temperature (Fig. 4C) reveals a sigmoidal transition during both heating and cooling.

Changes in average charge state (Fig. 4B) align closely with the temperature program (Fig. 4A). As the temperature increases, ubiquitin unfolds, and the average charge state increases; and the reverse occurs during cooling. Comparing the three thermal cycles of

ubiquitin, the behaviour of the unfolding and refolding curves remains highly consistent. Plotting average charge state versus temperature (Fig. 4C) shows that the curves overlap with repeated thermal cycling and the unfolding of ubiquitin remains highly reversible. Analysis of the T_m reveals that as the number of cycles increases, the T_m remains within ±1.3 °C. The outlier datapoints in the average charge state plots are due to fluctuations in ion current that are carried through the data workup and can affect the calculation of T_m.

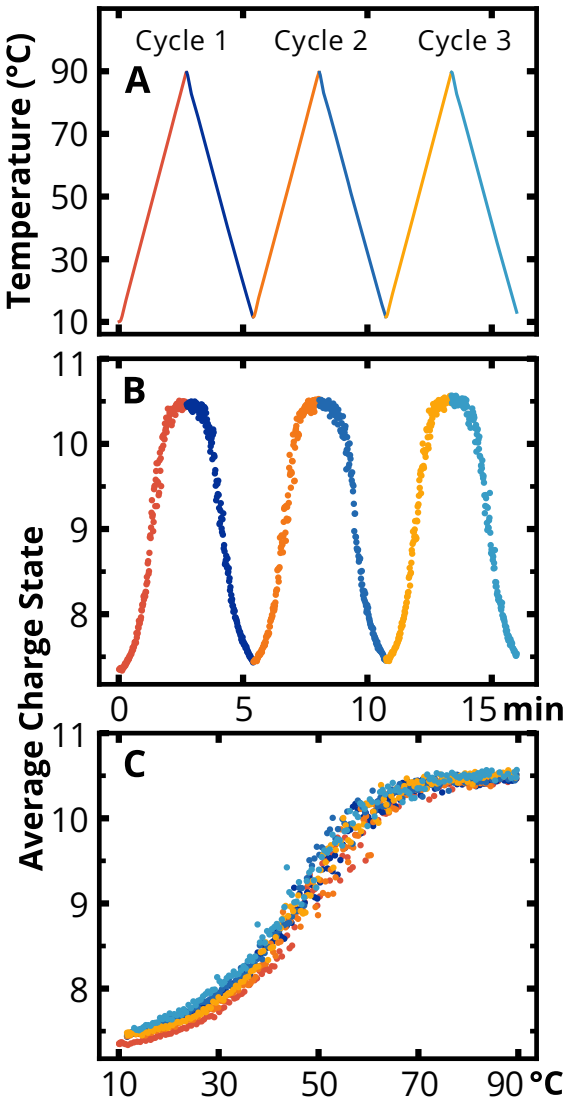

Figure 4. Three thermal cycles of ubiquitin at 30 °C·min^{-1}. The heating phase is in red-orange and the cooling phase is in blue. A) The block temperature for three thermal cycles, reflecting the

programmed temperature. B) The average charge state of ubiquitin changes with thermal cycles over time. The shape and timing matches the temperature program in A. C) The average charge state plotted versus temperature, revealing the sigmoidal shape of the transition.

Scan Rate Dependence of Lysozyme

Figure 5A shows the temperature program for three thermal cycles at a rate of ±30 °C·min^{-1}. For three cycles of ubiquitin (Fig. 5B), the average charge state as a function of temperature during heating (unfolding curve) and cooling (refolding curve) exhibit significant overlap. Note that the average charge state continues to return to the initial value at low temperature with increasing numbers of cycles. Lysozyme (Fig. 5C) has similarly consistent refolding, as the average charge state also continues to return to the initial low value with increasing cycles. However, the T_m shifts to lower temperatures with increasing numbers of cycles (Table S1). The ΔT_m remains present in all cycles.

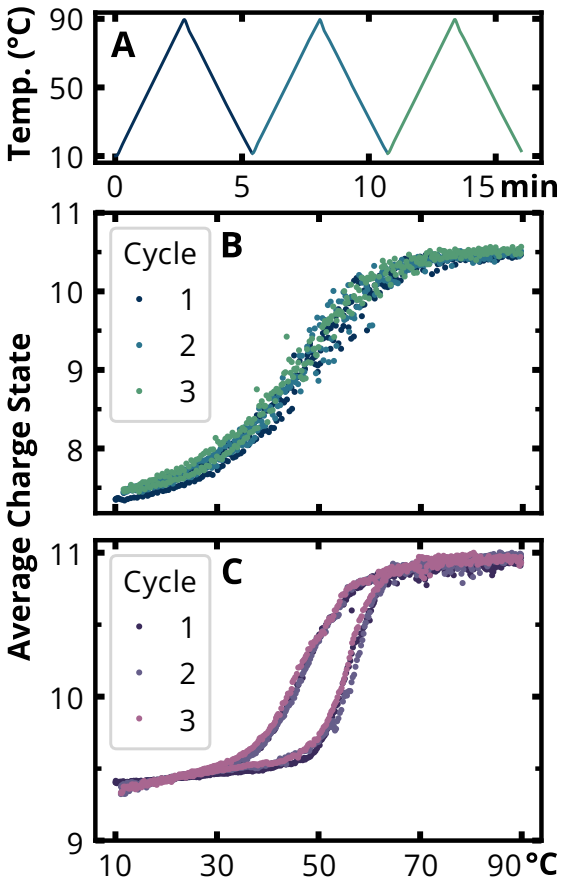

Figure 5. Three thermal cycles of ubiquitin and lysozyme. A) The block temperature for three thermal cycles of ubiquitin, reflecting the programmed temperature. The block temperature for lysozyme cycles is indistinguishable. B) Average charge state data for three cycles of ubiquitin. The curves for all three cycles overlap. C) Average charge state data for three cycles of lysozyme. There is a significant difference between the heating and cooling curves and ΔT_m is maintained over the repeated cycles.

Both ubiquitin and lysozyme (Fig. 5B and C), have highly reversible unfolding with repeated thermal cycling, indicating high thermal stability. In contrast to ubiquitin, lysozyme exhibits changes during the folding transitions. The T_m for both unfolding and refolding shifts to lower temperatures with repeated cycling. One possible explanation for this result is that the

sample pH decreases during these long electrospray experiments due to the oxidation of water.[54,55] It is known that T_m of proteins are dependent on solution pH. For aqueous lysozyme, it was found that the T_m shifts ~20 °C between pH 2 and 2.5 (Fig. S6). At ±30 °C·min^{-1}, it is less likely that acidification of the sample would occur, as three cycles takes ~15 min (Fig. 5C). However at ±9 °C·min^{-1} (Fig. 6A), three cycles takes ~50 min, a duration of time during which pH drift can occur.[55] If acidification is occurring, the T_m of the third cycle would be significantly lower during the longer experiments. Comparison of T_m from 30 and 9 °C·min^{-1} experiments reveals no significant difference. Gadzuk-Shea and coworkers observed acidification of samples that were initially at neutral pH.[55] The lysozyme samples in this experiment are at pH 2, i.e., initially have a proton concentration that is 10^5-fold higher, therefore the formation of additional protons by the oxidation of water would have a much smaller effect on pH. Cycling at the highest scan rate, 30 °C·min^{-1}, for the duration of the lowest rate experiment, 50 minutes, gives a 10-cycle experiment (Fig. S7) in which the T_m initially shifts to lower temperatures, but then shifts back to slightly higher temperatures. Additionally, the T_m of the cooling phase shows a more significant shift to lower temperatures compared to the T_m of the heating phase (Fig. S8).

While T_m is a useful metric for comparing results between different scan rates, or for measuring the effect of binding partners, it is less useful for characterizing changes between cycles within a single experiment. There is vastly more structural data being acquired that is not being used when solely using T_m as a metric, especially with ptESI. It is also sensitive to large fluctuations in ion current. The ion current changes with temperature (Fig. S3), which requires further investigation.

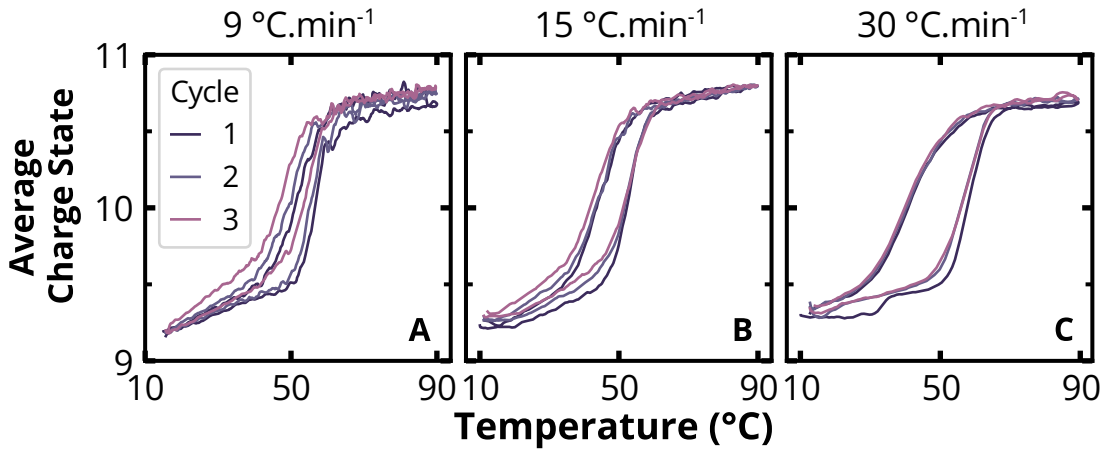

Figure 6. Three thermal cycles of lysozyme at three different scan rates. A) Three cycles at ±9 °C·min^{-1}. B) Three cycles at ±15 °C·min^{-1}. C) Three cycles at ±30 °C·min^{-1}. These plots have Savitsky-Golay[56] smoothing function applied for easier visualization of multiple overlaid cycles.

Figure 6 shows three-cycle experiments at ±9 (Fig. 6A), ±15 (Fig. 6B), and ±30 °C·min^{-1} (Fig. 6C). ΔT_m is present for all scan rates investigated and increases with increasing scan rate. The T_m values for both unfolding and refolding tend to shift to higher temperatures with increasing scan rate and are tabulated in Table S2.

The changes in T_m and ΔT_m indicate a scan rate dependence for thermal cycling of lysozyme. Scan rate dependence indicates that the scan rate is faster than the rate of unfolding and the protein is not at equilibrium, thus there is a kinetic component to the transition.[19] For small proteins like lysozyme, the rate of folding is assumed to be fast, but the observed scan rate dependence implies the rate is slower than assumed. Scan rates used in DSC are slow compared to ptESI, but scan rate dependence still occurs. In the case of lysozyme at low pH, it was found that folding occurs slower than at neutral pH and this was attributed to a kinetic intermediate state.[25] The changes in ΔT_m with scan rate may be due to a lag in protein refolding as mentioned

previously. The refolding is potentially frustrated due to tangles in the polypeptide chain and disulfide bonds. As the scan rate increases, the protein will likely take the same length of time to refold. The temperature is changing much faster than the protein is able to refold, this introduces as lag resulting in the ΔT_m increasing as the scan rate increases. At high temperatures, the asymptotic region has a closer overlap between the two curves and both curves reach this region at a similar temperature. The protein is in a disordered, conformationally heterogeneous state and the lag in refolding is less visible. At low temperatures, the unfolding and refolding curves do not overlap in the asymptotic region to the same extent and reach this region at different temperatures. The protein is in a more ordered, conformationally homogeneous state, and the lag in refolding is apparent. Even for a highly reversible system like lysozyme, it is important to consider kinetic effects and measuring at different scan rates can reveal scan rate dependencies.

Using ptESI with Multiplexing

Figure 7 shows data from multiplexed experiments of ubiquitin and lysozyme at pH 2.15. The curves for ubiquitin and lysozyme are overlaid (Fig. 7B), demonstrating the differences in average charge states between the two analytes.

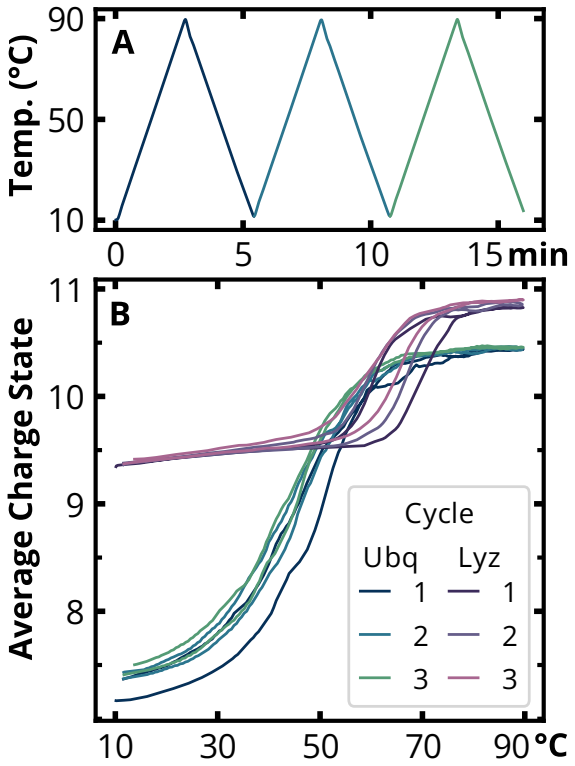

Figure 7. Multiplexed thermal cycling experiment with equimolar ubiquitin and lysozyme. A) The programmed temperature is reflected in the block temperature during three thermal cycles at a scan rate of ±30 °C·min^{-1}. B) Average charge state data for both ubiquitin (blue) and lysozyme (purple).

A strength of MS-based measurements is the ability to perform multiplexed experiments, which can also apply to tcESI.[43,46] The solutions of ubiquitin and lysozyme were prepared at the working pH for ubiquitin, as it is much more pH sensitive than lysozyme. This results in a minor shift of the lysozyme curves to higher temperatures (Fig. 7B). The T_m value for ubiquitin obtained from the multiplexed experiment is 44.8 ± 4.2 °C, which agrees with the values obtained in this study. The difference between the first unfolding curve of ubiquitin and all subsequent curves is due to a decrease in intensity at low temperatures in the ion chromatogram,

which is carried through the workup. The T_m values for lysozyme (Table S3) are higher than other results reported here, but this is attributed to the change in solution pH. Interestingly, the ΔT_m appears smaller than previous thermal cycles at 30 °C·min^{-1}. This may also be due to the higher pH being less destabilizing or less time spent at elevated temperatures during which the unfolded regions could get tangled. The greater change in average charge state for ubiquitin is very clearly demonstrated when lysozyme data is overlaid. Ubiquitin average charge state ranges from 7.5 – 10.5 over the course of a thermal cycle, whereas lysozyme only ranges between 9 – 11. The smaller change in average charge state likely also contributes to the ease in which lysozyme can be captured in the desired temperature range.

Conclusions

ptESI-MS is a powerful tool for thermal denaturation studies, in which large amounts of structural information is rapidly collected. It can scan across a broad range of temperatures while mass spectra are continuously acquired. In this work, we demonstrated the use of ptESI to study the thermal denaturation of model proteins using thermal cycling. At low pH, both ubiquitin and lysozyme have highly reversible transitions (Fig. 3). With repeated thermal cycling, ubiquitin exhibited overlapping unfolding and refolding curves and no scan rate dependence (Fig. 4), indicating it is in equilibrium during scanning. In contrast, thermal cycling of lysozyme (Fig. 5) revealed significant differences between the unfolding and refolding curves (ΔT_m), implying the refolding is frustrated and occurring slower than the unfolding. This may be due to unfolded regions becoming tangled in loops formed by disulfide bonds. Varying the scan rate (Fig. 6) and noting changes in T_m revealed a scan rate dependence, indicating there is a kinetic component to the transition between the native folded and denatured unfolded states of lysozyme. This work

also demonstrates the need to consider kinetic effects for reversible transitions, which can be exposed by investigating multiple scan rates. Multiplexed experiments can be performed using ptESI, as shown in Figure 7, but it requires proteins that are stable in the same solution conditions.

Compared to DSC, DSF, and CD, ptESI obtains more structural information in less time. T_m can be rapidly determined without the addition of dye like DSF, or large amounts of sample like DSC, but cannot monitor specific structural features like CD. More studies are needed to understand what is causing the scan rate dependence in ptESI. In this study, ubiquitin exhibited thermodynamic stability, as it remained in equilibrium throughout the experiment. For proteins like lysozyme, which exhibit a scan rate dependence and kinetic stability, there are options in experiment design to obtain equilibrium values: one could slow the scan rate until the scan rate dependence is eliminated, or one could use multiple fast scan rates to determine the dependence of T_m on scan rate and extrapolate a T_m at zero scan rate.[12] However, it may not be possible to fully eliminate kinetic effects, depending on the analyte. T_m is a useful metric for comparing stability between measurement techniques or for assessing the effects of a binding partner, but for evaluating folding behaviour between repeated thermal cycles in a single experiment it is lacking. For ptESI experiments in particular, a metric that makes better use of the wealth of mass spectral data acquired is needed.

Acknowledgements

This work was supported by the National Science Foundation through award 2203513 from the Division of Chemistry, with partial co-funding from the Division of Molecular and Cellular Biosciences.

References

(1) Anfinsen, C. B. Principles That Govern the Folding of Protein Chains. *Science* **1973**, *181* (4096), 223–230.

(2) Hingorani, K. S.; Gierasch, L. M. Comparing Protein Folding In Vitro and In Vivo: Foldability Meets the Fitness Challenge. *Curr. Opin. Struct. Biol.* **2014**, *0*, 81–90. https://doi.org/10.1016/j.sbi.2013.11.007.

(3) Creighton, T. E. Protein Folding. *Biochem. J.* **1990**, *270* (1), 1–16.

(4) Privalov, P. L.; Khechinashvili, N. N. A Thermodynamic Approach to the Problem of Stabilization of Globular Protein Structure: A Calorimetric Study. *J. Mol. Biol.* **1974**, *86* (3), 665–684. https://doi.org/10.1016/0022-2836(74)90188-0.

(5) Privalov, P. L.; Dragan, A. I. Microcalorimetry of Biological Macromolecules. *Biophys. Chem.* **2007**, *126* (1–3), 16–24. https://doi.org/10.1016/j.bpc.2006.05.004.

(6) Chaires, J. B. Calorimetry and Thermodynamics in Drug Design. *Annu. Rev. Biophys.* **2008**, *37* (1), 135–151. https://doi.org/10.1146/annurev.biophys.36.040306.132812.

(7) Jacobson, A. L.; Braun, H. Differential Scanning Calorimetry of the Thermal Denaturation of Lactate Dehydrogenase. *Biochim. Biophys. Acta BBA - Protein Struct.* **1977**, *493* (1), 142–153. https://doi.org/10.1016/0005-2795(77)90267-7.

(8) Vagenende, V.; Yap, M. G. S.; Trout, B. L. Mechanisms of Protein Stabilization and Prevention of Protein Aggregation by Glycerol. *Biochemistry* **2009**, *48* (46), 11084–11096. https://doi.org/10.1021/bi900649t.

(9) Gaisford, S. Fast-Scan Differential Scanning Calorimetry. *Eur. Pharm. Rev.*

(10) Mukhametzyanov, T. A.; Sedov, I. A.; Solomonov, B. N.; Schick, C. Fast Scanning Calorimetry of Lysozyme Unfolding at Scanning Rates from 5 K/Min to 500,000 K/Min.

Biochim. Biophys. Acta BBA - Gen. Subj. **2018**, *1862* (9), 2024–2030. https://doi.org/10.1016/j.bbagen.2018.06.019.

(11) Garbett, N. C.; Chaires, J. B. Thermodynamic Studies for Drug Design and Screening. *Expert Opin. Drug Discov.* **2012**, *7* (4), 299–314. https://doi.org/10.1517/17460441.2012.666235.

(12) Lang, B. E.; Cole, K. D. Differential Scanning Calorimetry and Fluorimetry Measurements of Monoclonal Antibodies and Reference Proteins: Effect of Scanning Rate and Dye Selection. *Biotechnol. Prog.* **2017**, *33* (3), 677–686. https://doi.org/10.1002/btpr.2464.

(13) Niesen, F. H.; Berglund, H.; Vedadi, M. The Use of Differential Scanning Fluorimetry to Detect Ligand Interactions That Promote Protein Stability. *Nat. Protoc.* **2007**, *2* (9), 2212–2221. https://doi.org/10.1038/nprot.2007.321.

(14) He, F.; Hogan, S.; Latypov, R. F.; Narhi, L. O.; Razinkov, V. I. High Throughput Thermostability Screening of Monoclonal Antibody Formulations. *J. Pharm. Sci.* **2010**, *99* (4), 1707–1720. https://doi.org/10.1002/jps.21955.

(15) Greenfield, N. J. Using Circular Dichroism Collected as a Function of Temperature to Determine the Thermodynamics of Protein Unfolding and Binding Interactions. *Nat. Protoc.* **2006**, *1* (6), 2527–2535. https://doi.org/10.1038/nprot.2006.204.

(16) Sreerama, N.; Venyaminov, S. Yu.; Woody, R. W. Estimation of Protein Secondary Structure from Circular Dichroism Spectra: Inclusion of Denatured Proteins with Native Proteins in the Analysis. *Anal. Biochem.* **2000**, *287* (2), 243–251. https://doi.org/10.1006/abio.2000.4879.

(17) Kelly, S. M.; Price, N. C. The Application of Circular Dichroism to Studies of Protein Folding and Unfolding. *Biochim. Biophys. Acta BBA - Protein Struct. Mol. Enzymol.* **1997**, *1338* (2), 161–185. https://doi.org/10.1016/S0167-4838(96)00190-2.

(18) Davoodi, J.; Wakarchuk, W. W.; Surewicz, W. K.; Carey, P. R. Scan-rate dependence in protein calorimetry: The reversible transitions of Bacillus circulans xylanase and a disulfide-bridge mutant. *Protein Sci.* **1998**, *7* (7), 1538–1544. https://doi.org/10.1002/pro.5560070707.

(19) Lepock, J. R.; Ritchie, K. P.; Kolios, M. C.; Rodahl, A. M.; Heinz, K. A.; Kruuv, J. Influence of Transition Rates and Scan Rate on Kinetic Simulations of Differential Scanning Calorimetry Profiles of Reversible and Irreversible Protein Denaturation. *Biochemistry* **1992**, *31* (50), 12706–12712. https://doi.org/10.1021/bi00165a023.

(20) Damgaard, R. B. The Ubiquitin System: From Cell Signalling to Disease Biology and New Therapeutic Opportunities. *Cell Death Differ.* **2021**, *28* (2), 423–426. https://doi.org/10.1038/s41418-020-00703-w.

(21) Jackson, S. E. Ubiquitin: A Small Protein Folding Paradigm. *Org. Biomol. Chem.* **2006**, *4* (10), 1845–1853. https://doi.org/10.1039/B600829C.

(22) Wintrode, P. L.; Makhatadze, G. I.; Privalov, P. L. Thermodynamics of Ubiquitin Unfolding. *Proteins* **1994**, *18* (3), 246–253. https://doi.org/10.1002/prot.340180305.

(23) Kugimiya, M.; Bigelow, C. C. The Denatured States of Lysozyme. *Can. J. Biochem.* **1973**, *51* (5), 581–585. https://doi.org/10.1139/o73-072.

(24) Lee, J. W.; Kim, H. I. Investigating Acid-Induced Structural Transitions of Lysozyme in an Electrospray Ionization Source. *The Analyst* **2015**, *140* (2), 661–669. https://doi.org/10.1039/C4AN01794C.

(25) Sasahara, K.; Demura, M.; Nitta, K. Equilibrium and Kinetic Folding of Hen Egg-White Lysozyme under Acidic Conditions. *Proteins Struct. Funct. Bioinforma.* **2002**, *49* (4), 472–482. https://doi.org/10.1002/prot.10215.

(26) Leney, A. C.; Heck, A. J. R. Native Mass Spectrometry: What Is in the Name? *J. Am. Soc. Mass Spectrom.* **2017**, *28* (1), 5–13. https://doi.org/10.1007/s13361-016-1545-3.

(27) Wang, G.; Abzalimov, R. R.; Kaltashov, I. A. Direct Monitoring of Heat-Stressed Biopolymers with Temperature-Controlled Electrospray Ionization Mass Spectrometry. *Anal. Chem.* **2011**, *83* (8), 2870–2876. https://doi.org/10.1021/ac200441a.

(28) Mirza, U. A.; Cohen, S. L.; Chait, B. T. Heat-Induced Conformational Changes in Proteins Studied by Electrospray Ionization Mass Spectrometry. *Anal. Chem.* **1993**, *65* (1), 1–6. https://doi.org/10.1021/ac00049a003.

(29) Benesch, J. L. P.; Sobott, F.; Robinson, C. V. Thermal Dissociation of Multimeric Protein Complexes by Using Nanoelectrospray Mass Spectrometry. *Anal. Chem.* **2003**, *75* (10), 2208–2214. https://doi.org/10.1021/ac034132x.

(30) Geels, R. B. J.; Calmat, S.; Heck, A. J. R.; van der Vies, S. M.; Heeren, R. M. A. Thermal Activation of the Co-Chaperonins GroES and Gp31 Probed by Mass Spectrometry. *Rapid Commun. Mass Spectrom.* **2008**, *22* (22), 3633–3641. https://doi.org/10.1002/rcm.3782.

(31) Cong, X.; Liu, Y.; Liu, W.; Liang, X.; Russell, D. H.; Laganowsky, A. Determining Membrane Protein–Lipid Binding Thermodynamics Using Native Mass Spectrometry. *J. Am. Chem. Soc.* **2016**, *138* (13), 4346–4349. https://doi.org/10.1021/jacs.6b01771.

(32) Lippens, J. L.; Mangrum, J. B.; McIntyre, W.; Redick, B.; Fabris, D. A Simple Heated-Capillary Modification Improves the Analysis of Non-Covalent Complexes by Z-Spray

Electrospray Ionization. *Rapid Commun. Mass Spectrom.* **2016**, *30* (6), 773–783. https://doi.org/10.1002/rcm.7490.

(33) El-Baba, T. J.; Woodall, D. W.; Raab, S. A.; Fuller, D. R.; Laganowsky, A.; Russell, D. H.; Clemmer, D. E. Melting Proteins: Evidence for Multiple Stable Structures upon Thermal Denaturation of Native Ubiquitin from Ion Mobility Spectrometry-Mass Spectrometry Measurements. *J. Am. Chem. Soc.* **2017**, *139* (18), 6306–6309. https://doi.org/10.1021/jacs.7b02774.

(34) El-Baba, T. J.; Clemmer, D. E. Solution Thermochemistry of Concanavalin A Tetramer Conformers Measured by Variable-Temperature ESI-IMS-MS. *Int. J. Mass Spectrom.* **2019**, *443*, 93–100. https://doi.org/10.1016/j.ijms.2019.06.004.

(35) McCabe, J. W.; Shirzadeh, M.; Walker, T. E.; Lin, C.-W.; Jones, B. J.; Wysocki, V. H.; Barondeau, D. P.; Clemmer, D. E.; Laganowsky, A.; Russell, D. H. Variable-Temperature Electrospray Ionization for Temperature-Dependent Folding/Refolding Reactions of Proteins and Ligand Binding. *Anal. Chem.* **2021**, *93* (18), 6924–6931. https://doi.org/10.1021/acs.analchem.1c00870.

(36) Hommersom, B.; Porta, T.; Heeren, R. M. A. Ion Mobility Spectrometry Reveals Intermediate States in Temperature-Resolved DNA Unfolding. *Int. J. Mass Spectrom.* **2017**, *419*, 52–55. https://doi.org/10.1016/j.ijms.2017.03.008.

(37) Marchand, A.; Rosu, F.; Zenobi, R.; Gabelica, V. Thermal Denaturation of DNA G-Quadruplexes and Their Complexes with Ligands: Thermodynamic Analysis of the Multiple States Revealed by Mass Spectrometry. *J. Am. Chem. Soc.* **2018**, *140* (39), 12553–12565. https://doi.org/10.1021/jacs.8b07302.

(38) Pruška, A.; Marchand, A.; Zenobi, R. Novel Insight into Proximal DNA Domain Interactions from Temperature-Controlled Electrospray Ionization Mass Spectrometry. *Angew. Chem. Int. Ed.* **2021**, *60* (28), 15390–15398. https://doi.org/10.1002/anie.202016757.

(39) Liu, J.; Wang, Y.; Wang, X.; Qin, W.; Li, G. Measuring Protein Unfolding Thermodynamic Stability in One Minute with Digital Temperature Control-Equipped nanoESI-Mass Spectrometry. *Int. J. Mass Spectrom.* **2023**, *494*, 117151. https://doi.org/10.1016/j.ijms.2023.117151.

(40) Daneshfar, R.; Kitova, E. N.; Klassen, J. S. Determination of Protein−Ligand Association Thermochemistry Using Variable-Temperature Nanoelectrospray Mass Spectrometry. *J. Am. Chem. Soc.* **2004**, *126* (15), 4786–4787. https://doi.org/10.1021/ja0316972.

(41) Raab, S. A.; El-Baba, T. J.; Woodall, D. W.; Liu, W.; Liu, Y.; Baird, Z.; Hales, D. A.; Laganowsky, A.; Russell, D. H.; Clemmer, D. E. Evidence for Many Unique Solution Structures for Chymotrypsin Inhibitor 2: A Thermodynamic Perspective Derived from vT-ESI-IMS-MS Measurements. *J. Am. Chem. Soc.* **2020**, *142* (41), 17372–17383. https://doi.org/10.1021/jacs.0c05365.

(42) Woodall, D. W.; Henderson, L. W.; Raab, S. A.; Honma, K.; Clemmer, D. E. Understanding the Thermal Denaturation of Myoglobin with IMS-MS: Evidence for Multiple Stable Structures and Trapped Pre-Equilibrium States. *J. Am. Soc. Mass Spectrom.* **2021**, *32* (1), 64–72. https://doi.org/10.1021/jasms.0c00075.

(43) Jordan, J. S.; Williams, E. R. Laser Heating Nanoelectrospray Emitters for Fast Protein Melting Measurements with Mass Spectrometry. *Anal. Chem.* **2022**, *94* (48), 16894–16900. https://doi.org/10.1021/acs.analchem.2c04204.

(44) Laszlo, K. J.; Buckner, J. H.; Munger, E. B.; Bush, M. F. Native-Like and Denatured Cytochrome *c* Ions Yield Cation-to-Anion Proton Transfer Reaction Products with Similar Collision Cross-Sections. *J. Am. Soc. Mass Spectrom.* **2017**, *28* (7), 1382–1391. https://doi.org/10.1007/s13361-017-1620-4.

(45) Leney, A. C.; Heck, A. J. R. Native Mass Spectrometry: What Is in the Name? *J. Am. Soc. Mass Spectrom.* **2017**, *28* (1), 5–13. https://doi.org/10.1007/s13361-016-1545-3.

(46) El-Baba, T. J.; Raab, S. A.; Buckley, R. P.; Brown, C. J.; Lutomski, C. A.; Henderson, L. W.; Woodall, D. W.; Shen, J.; Trinidad, J. C.; Niu, H.; Jarrold, M. F.; Russell, D. H.; Laganowsky, A.; Clemmer, D. E. Thermal Analysis of a Mixture of Ribosomal Proteins by vT-ESI-MS: Toward a Parallel Approach for Characterizing the Stabilitome. *Anal. Chem.* **2021**, *93* (24), 8484–8492. https://doi.org/10.1021/acs.analchem.1c00772.

(47) Giles, K.; Ujma, J.; Wildgoose, J.; Pringle, S.; Richardson, K.; Langridge, D.; Green, M. A Cyclic Ion Mobility-Mass Spectrometry System. *Anal. Chem.* **2019**, *91* (13), 8564–8573. https://doi.org/10.1021/acs.analchem.9b01838.

(48) Aune, K. C.; Salahuddin, A.; Zarlengo, M. H.; Tanford, C. Evidence for Residual Structure in Acid- and Heat-Denatured Proteins. *J. Biol. Chem.* **1967**, *242* (19), 4486–4489. https://doi.org/10.1016/S0021-9258(18)99563-3.

(49) Haezebrouck, P.; Joniau, M.; Van Dael, H.; Hooke, S. D.; Woodruff, N. D.; Dobson, C. M. An Equilibrium Partially Folded State of Human Lysozyme at Low pH. *J. Mol. Biol.* **1995**, *246* (3), 382–387. https://doi.org/10.1006/jmbi.1994.0093.

(50) Tanford, C.; Aune, K. C.; Ikai, A. Kinetics of Unfolding and Refolding of Proteins: III. Results for Lysozyme. *J. Mol. Biol.* **1973**, *73* (2), 185–197. https://doi.org/10.1016/0022-2836(73)90322-7.

(51) Kuwajima, K.; Hiraoka, Y.; Ikeguchi, M.; Sugai, S. Comparison of the Transient Folding Intermediates in Lysozyme and .Alpha.-Lactalbumin. *Biochemistry* **1985**, *24* (4), 874–881. https://doi.org/10.1021/bi00325a010.

(52) Kiefhaber, T. Kinetic Traps in Lysozyme Folding. *Proc. Natl. Acad. Sci.* **1995**, *92* (20), 9029–9033. https://doi.org/10.1073/pnas.92.20.9029.

(53) Kotov, V.; Mlynek, G.; Vesper, O.; Pletzer, M.; Wald, J.; Teixeira-Duarte, C. M.; Celia, H.; Garcia-Alai, M.; Nussberger, S.; Buchanan, S. K.; Morais-Cabral, J. H.; Loew, C.; Djinovic-Carugo, K.; Marlovits, T. C. In-Depth Interrogation of Protein Thermal Unfolding Data with MoltenProt. *Protein Sci.* **2021**, *30* (1), 201–217. https://doi.org/10.1002/pro.3986.

(54) Van Berkel, G. J.; Asano, K. G.; Schnier, P. D. Electrochemical Processes in a Wire-in-a-Capillary Bulk-Loaded, Nano-Electrospray Emitter. *J. Am. Soc. Mass Spectrom.* **2001**, *12* (7), 853–862. https://doi.org/10.1016/S1044-0305(01)00264-1.

(55) Gadzuk-Shea, M. M.; Hubbard, E. E.; Gozzo, T. A.; Bush, M. F. Sample pH Can Drift during Native Mass Spectrometry Experiments: Results from Ratiometric Fluorescence Imaging. *J. Am. Soc. Mass Spectrom.* **2023**, *34* (8), 1675–1684. https://doi.org/10.1021/jasms.3c00147.

(56) Savitzky, Abraham.; Golay, M. J. E. Smoothing and Differentiation of Data by Simplified Least Squares Procedures. *Anal. Chem.* **1964**, *36* (8), 1627–1639. https://doi.org/10.1021/ac60214a047.

(57) Creighton, T. E. The Energetic Ups and Downs of Protein Folding. *Nat. Struct. Biol.* **1994**, *1* (3), 135–138. https://doi.org/10.1038/nsb0394-135.

(58) Gozzo, T. A.; Weir, C. J.; Constabel, M. A.; Bush, M. F. Selecting Reducing Agents for Native Mass Spectrometry. ChemRxiv February 1, 2024. https://doi.org/10.26434/chemrxiv-2024-2nmh4-v2.

(59) Duckworth, H. W.; Nguyen, N. T.; Gao, Y.; Donald, L. J.; Maurus, R.; Ayed, A.; Bruneau, B.; Brayer, G. D. Enzyme–Substrate Complexes of Allosteric Citrate Synthase: Evidence for a Novel Intermediate in Substrate Binding. *Biochim. Biophys. Acta BBA - Proteins Proteomics* **2013**, *1834* (12), 2546–2553. https://doi.org/10.1016/j.bbapap.2013.07.019.

(60) Bai, J.-H.; Wang, H.-J.; Liu, D.-S.; Zhou, H.-M. Kinetics of Thermal Inactivation of Lactate Dehydrogenase from Rabbit Muscle. *J. Protein Chem. 16* (8).

CHAPTER III

Conclusions

In this study, the novel technique ptESI is used to characterize the thermally induced unfolding and refolding of two model proteins: ubiquitin and lysozyme. ptESI offers many advantages over traditional thermal techniques like DSC, DSF, and CD because of its speed, thermal cycling capabilities, and the large quantities of structural data that can be obtained. The experimental results provide insight into some of the folding processes of two model proteins and the differences between them.

An early goal of this work was to characterize the source and the data that can be acquired with it, as the source was designed and built by Dr. Meagan Gadzuk-Shea, who graduated several years prior. As we gained experience using the source and acquiring data with it, the extent of what can be done with ptESI began to be revealed. A strength of ptESI is the sheer amount of data that can be collected in very short amounts of time. Compared to tcESI experiments, ptESI experiments continuously acquire mass spectra while the temperature is changed, and is capable of thermal cycling. This results in rapid, data dense experiments.

Ubiquitin showed highly reversible unfolding and refolding transitions. The results do not indicate a scan rate dependence, suggesting that ubiquitin is at equilibrium throughout the measurement. Thermal cycles demonstrate the reversibility of the unfolding, and the lack of ΔT_m indicates refolding is proceeding unhindered. Ubiquitin appears to be highly sensitive to pH, as very small changes in pH resulted in large shifts in T_m. The pH sensitivity combined with the moderate slope of the unfolding transition created challenges obtaining a full sigmoidal transition

within the optimal operating temperatures of the ptESI source (10 – 90 ˚C). Ubiquitin exhibited very stable behaviour and is contrasted by lysozyme.

Lysozyme also showed highly reversible unfolding, but in contrast to ubiquitin, the results show a scan rate dependence, suggesting that the protein is not at equilibrium during the unfolding and refolding transitions. We tend to assume that small proteins like lysozyme fold fast relative to the scan rate, but T_m and ΔT_m increasing with increasing scan rate imply that there is a kinetic component to the transitions. The presence of ΔT_m implies a difference in the unfolding and refolding processes, likely arising due to refolding being more complex.[57] It may be due to unfolded regions becoming tangled in loops formed by disulfide bonds,[52] as the disulfide bonds are likely maintained at elevated temperature. Throughout the various thermal cycling experiments, the refolding remained highly reversible, highlighting that even reversible transitions can show scan rate dependence. When studying a new protein, I recommend investigating multiple scan rates as this can reveal scan rate dependencies and kinetic effects.

ptESI is limited to temperatures between 0 – 100 ˚C to avoid freezing or boiling the sample in the capillary. In practice, this generally means remaining between 3 – 97 ˚C. As model proteins have historically been chosen for their stability, many of them – including ubiquitin and lysozyme – do not have unfolding transitions within this temperature range. Thus, to obtain a reasonable T_m the protein is first destabilized using pH. While the stability of these proteins contributed to their adoption as model systems, it forces the use of non-physiological pH values to obtain a visible transition. The work presented here furthers our understanding of folding and its study using fast-scanning methods, but the protein-specific findings will not fully relate to what occurs at physiological pH. Furthermore, working at such low pH limits what reagents can be used. For example, the reducing agent dithiothreitol (DTT) does not work in this pH range

and cannot be used to further investigate the possibility of disulfide scrambling. Another commonly used reducing agent, tris(2-carboxyethyl)phosphine (TCEP), can be used at low pH, but it is proposed to be a powerful charge-reducing agent in native MS and would therefore be incompatible with this study.[58] The ptESI source can scan at rates of up to 120 ˚C·min^{-1}, but in practice it is limited by the rate of mass spectral acquisition, as discussed in Liu et al.[39] If the temperature is scanned faster than mass spectra can be acquired, the temperature resolution is lost. To a certain extent, the scan acquisition time can be shortened, at the sacrifice of signal-to-noise.

Average charge state is weighted by the intensity of the peaks, however in ptESI the peak intensity fluctuates with the ion current, which appears to fluctuate with temperature. In non-ptESI experiments, the ion current is generally very stable. Further investigation into the effects of temperature on ESI is needed to aid our understanding of the source of the ion current fluctuations. T_m is calculated through a curve fit applied to the plot of average charge state versus temperature and is thus also dependent on ion current fluctuations. While T_m is a good metric for comparing to established methods or between scan rates, the complexities of repeated thermal cycling experiments and ion current fluctuations mean it is not the most well-suited for comparing cycles within the same experiment. While average charge state plots present data in a simple and easily understandable format that clearly demonstrates unfolding, it does not adequately represent the vast amount of structural data obtained, especially in the more data dense ptESI experiments.

ptESI is an exciting new technology. In the future, we want to build on the work shown study proteins that are expected to have an unfolding transition between 5 – 95 ˚C at neutral pH such as citrate synthase, lactate dehydrogenase, and α-lactalbumin. The potentially frustrated

refolding exhibited by acidified lysozyme warrants further investigations on the effects of disulfide bonds on refolding. α-lactalbumin is homologous in sequence to lysozyme[51] and also has 4 disulfide bonds, but can be studied at neutral pH, where DTT can be used. Preliminary work has already begun on α-lactalbumin, but the slope of the transition may be too gentle for a strong sigmoidal transition in the temperature range of ptESI. A powerful use of the ptESI source would be for binding assays, analogous to those often performed using DSF, but with potentially far more information content. The ability of a binding partner, like a drug candidate molecule, to stabilize or destabilize a protein is reflected in large shifts in T_m. Citrate synthase is of interest as it can have multiple different small molecule binding partners.[59] Lactate dehydrogenase can also bind small molecules, forms oligomers, and previous studies have shown that substrate binding may help prevent thermal inactivation.[60] The fast scan rates of ptESI will allow for short experiment times and a high overall throughput, and could be very useful as part of drug development and screening for pharmaceuticals and biotherapeutics. Another vital component of bringing a therapeutic to market is stability testing, in which samples are held at elevated temperature for prolonged periods of time. ptESI may be able to provide an alternative method of "stress-testing" suitable biotherapeutics through rapid and repeated thermal cycling. Coupled to MS, sample degradation can be monitored in real-time. Overall, ptESI is a versatile technique that has the potential to be applied to studying fundamental interactions involved in protein folding and as part of routine testing during the development of biotherapeutics and drugs.

References

(1) Anfinsen, C. B. Principles That Govern the Folding of Protein Chains. *Science* **1973**, *181* (4096), 223–230.

(2) Hingorani, K. S.; Gierasch, L. M. Comparing Protein Folding In Vitro and In Vivo: Foldability Meets the Fitness Challenge. *Curr. Opin. Struct. Biol.* **2014**, *0*, 81–90. https://doi.org/10.1016/j.sbi.2013.11.007.

(3) Creighton, T. E. Protein Folding. *Biochem. J.* **1990**, *270* (1), 1–16.

(4) Privalov, P. L.; Khechinashvili, N. N. A Thermodynamic Approach to the Problem of Stabilization of Globular Protein Structure: A Calorimetric Study. *J. Mol. Biol.* **1974**, *86* (3), 665–684. https://doi.org/10.1016/0022-2836(74)90188-0.

(5) Privalov, P. L.; Dragan, A. I. Microcalorimetry of Biological Macromolecules. *Biophys. Chem.* **2007**, *126* (1–3), 16–24. https://doi.org/10.1016/j.bpc.2006.05.004.

(6) Chaires, J. B. Calorimetry and Thermodynamics in Drug Design. *Annu. Rev. Biophys.* **2008**, *37* (1), 135–151. https://doi.org/10.1146/annurev.biophys.36.040306.132812.

(7) Jacobson, A. L.; Braun, H. Differential Scanning Calorimetry of the Thermal Denaturation of Lactate Dehydrogenase. *Biochim. Biophys. Acta BBA - Protein Struct.* **1977**, *493* (1), 142–153. https://doi.org/10.1016/0005-2795(77)90267-7.

(8) Vagenende, V.; Yap, M. G. S.; Trout, B. L. Mechanisms of Protein Stabilization and Prevention of Protein Aggregation by Glycerol. *Biochemistry* **2009**, *48* (46), 11084–11096. https://doi.org/10.1021/bi900649t.

(9) Gaisford, S. Fast-Scan Differential Scanning Calorimetry. *Eur. Pharm. Rev.*

(10) Mukhametzyanov, T. A.; Sedov, I. A.; Solomonov, B. N.; Schick, C. Fast Scanning Calorimetry of Lysozyme Unfolding at Scanning Rates from 5 K/Min to 500,000 K/Min.

Biochim. Biophys. Acta BBA - Gen. Subj. **2018**, *1862* (9), 2024–2030. https://doi.org/10.1016/j.bbagen.2018.06.019.

(11) Garbett, N. C.; Chaires, J. B. Thermodynamic Studies for Drug Design and Screening. *Expert Opin. Drug Discov.* **2012**, *7* (4), 299–314. https://doi.org/10.1517/17460441.2012.666235.

(12) Lang, B. E.; Cole, K. D. Differential Scanning Calorimetry and Fluorimetry Measurements of Monoclonal Antibodies and Reference Proteins: Effect of Scanning Rate and Dye Selection. *Biotechnol. Prog.* **2017**, *33* (3), 677–686. https://doi.org/10.1002/btpr.2464.

(13) Niesen, F. H.; Berglund, H.; Vedadi, M. The Use of Differential Scanning Fluorimetry to Detect Ligand Interactions That Promote Protein Stability. *Nat. Protoc.* **2007**, *2* (9), 2212–2221. https://doi.org/10.1038/nprot.2007.321.

(14) He, F.; Hogan, S.; Latypov, R. F.; Narhi, L. O.; Razinkov, V. I. High Throughput Thermostability Screening of Monoclonal Antibody Formulations. *J. Pharm. Sci.* **2010**, *99* (4), 1707–1720. https://doi.org/10.1002/jps.21955.

(15) Greenfield, N. J. Using Circular Dichroism Collected as a Function of Temperature to Determine the Thermodynamics of Protein Unfolding and Binding Interactions. *Nat. Protoc.* **2006**, *1* (6), 2527–2535. https://doi.org/10.1038/nprot.2006.204.

(16) Sreerama, N.; Venyaminov, S. Yu.; Woody, R. W. Estimation of Protein Secondary Structure from Circular Dichroism Spectra: Inclusion of Denatured Proteins with Native Proteins in the Analysis. *Anal. Biochem.* **2000**, *287* (2), 243–251. https://doi.org/10.1006/abio.2000.4879.

(17) Kelly, S. M.; Price, N. C. The Application of Circular Dichroism to Studies of Protein Folding and Unfolding. *Biochim. Biophys. Acta BBA - Protein Struct. Mol. Enzymol.* **1997**, *1338* (2), 161–185. https://doi.org/10.1016/S0167-4838(96)00190-2.

(18) Davoodi, J.; Wakarchuk, W. W.; Surewicz, W. K.; Carey, P. R. Scan-rate dependence in protein calorimetry: The reversible transitions of Bacillus circulans xylanase and a disulfide-bridge mutant. *Protein Sci.* **1998**, *7* (7), 1538–1544. https://doi.org/10.1002/pro.5560070707.

(19) Lepock, J. R.; Ritchie, K. P.; Kolios, M. C.; Rodahl, A. M.; Heinz, K. A.; Kruuv, J. Influence of Transition Rates and Scan Rate on Kinetic Simulations of Differential Scanning Calorimetry Profiles of Reversible and Irreversible Protein Denaturation. *Biochemistry* **1992**, *31* (50), 12706–12712. https://doi.org/10.1021/bi00165a023.

(20) Damgaard, R. B. The Ubiquitin System: From Cell Signalling to Disease Biology and New Therapeutic Opportunities. *Cell Death Differ.* **2021**, *28* (2), 423–426. https://doi.org/10.1038/s41418-020-00703-w.

(21) Jackson, S. E. Ubiquitin: A Small Protein Folding Paradigm. *Org. Biomol. Chem.* **2006**, *4* (10), 1845–1853. https://doi.org/10.1039/B600829C.

(22) Wintrode, P. L.; Makhatadze, G. I.; Privalov, P. L. Thermodynamics of Ubiquitin Unfolding. *Proteins* **1994**, *18* (3), 246–253. https://doi.org/10.1002/prot.340180305.

(23) Kugimiya, M.; Bigelow, C. C. The Denatured States of Lysozyme. *Can. J. Biochem.* **1973**, *51* (5), 581–585. https://doi.org/10.1139/o73-072.

(24) Lee, J. W.; Kim, H. I. Investigating Acid-Induced Structural Transitions of Lysozyme in an Electrospray Ionization Source. *The Analyst* **2015**, *140* (2), 661–669. https://doi.org/10.1039/C4AN01794C.

(25) Sasahara, K.; Demura, M.; Nitta, K. Equilibrium and Kinetic Folding of Hen Egg-White Lysozyme under Acidic Conditions. *Proteins Struct. Funct. Bioinforma.* **2002**, *49* (4), 472–482. https://doi.org/10.1002/prot.10215.

(26) Leney, A. C.; Heck, A. J. R. Native Mass Spectrometry: What Is in the Name? *J. Am. Soc. Mass Spectrom.* **2017**, *28* (1), 5–13. https://doi.org/10.1007/s13361-016-1545-3.

(27) Wang, G.; Abzalimov, R. R.; Kaltashov, I. A. Direct Monitoring of Heat-Stressed Biopolymers with Temperature-Controlled Electrospray Ionization Mass Spectrometry. *Anal. Chem.* **2011**, *83* (8), 2870–2876. https://doi.org/10.1021/ac200441a.

(28) Mirza, U. A.; Cohen, S. L.; Chait, B. T. Heat-Induced Conformational Changes in Proteins Studied by Electrospray Ionization Mass Spectrometry. *Anal. Chem.* **1993**, *65* (1), 1–6. https://doi.org/10.1021/ac00049a003.

(29) Benesch, J. L. P.; Sobott, F.; Robinson, C. V. Thermal Dissociation of Multimeric Protein Complexes by Using Nanoelectrospray Mass Spectrometry. *Anal. Chem.* **2003**, *75* (10), 2208–2214. https://doi.org/10.1021/ac034132x.

(30) Geels, R. B. J.; Calmat, S.; Heck, A. J. R.; van der Vies, S. M.; Heeren, R. M. A. Thermal Activation of the Co-Chaperonins GroES and Gp31 Probed by Mass Spectrometry. *Rapid Commun. Mass Spectrom.* **2008**, *22* (22), 3633–3641. https://doi.org/10.1002/rcm.3782.

(31) Cong, X.; Liu, Y.; Liu, W.; Liang, X.; Russell, D. H.; Laganowsky, A. Determining Membrane Protein–Lipid Binding Thermodynamics Using Native Mass Spectrometry. *J. Am. Chem. Soc.* **2016**, *138* (13), 4346–4349. https://doi.org/10.1021/jacs.6b01771.

(32) Lippens, J. L.; Mangrum, J. B.; McIntyre, W.; Redick, B.; Fabris, D. A Simple Heated-Capillary Modification Improves the Analysis of Non-Covalent Complexes by Z-Spray

Electrospray Ionization. *Rapid Commun. Mass Spectrom.* **2016**, *30* (6), 773–783. https://doi.org/10.1002/rcm.7490.

(33) El-Baba, T. J.; Woodall, D. W.; Raab, S. A.; Fuller, D. R.; Laganowsky, A.; Russell, D. H.; Clemmer, D. E. Melting Proteins: Evidence for Multiple Stable Structures upon Thermal Denaturation of Native Ubiquitin from Ion Mobility Spectrometry-Mass Spectrometry Measurements. *J. Am. Chem. Soc.* **2017**, *139* (18), 6306–6309. https://doi.org/10.1021/jacs.7b02774.

(34) El-Baba, T. J.; Clemmer, D. E. Solution Thermochemistry of Concanavalin A Tetramer Conformers Measured by Variable-Temperature ESI-IMS-MS. *Int. J. Mass Spectrom.* **2019**, *443*, 93–100. https://doi.org/10.1016/j.ijms.2019.06.004.

(35) McCabe, J. W.; Shirzadeh, M.; Walker, T. E.; Lin, C.-W.; Jones, B. J.; Wysocki, V. H.; Barondeau, D. P.; Clemmer, D. E.; Laganowsky, A.; Russell, D. H. Variable-Temperature Electrospray Ionization for Temperature-Dependent Folding/Refolding Reactions of Proteins and Ligand Binding. *Anal. Chem.* **2021**, *93* (18), 6924–6931. https://doi.org/10.1021/acs.analchem.1c00870.

(36) Hommersom, B.; Porta, T.; Heeren, R. M. A. Ion Mobility Spectrometry Reveals Intermediate States in Temperature-Resolved DNA Unfolding. *Int. J. Mass Spectrom.* **2017**, *419*, 52–55. https://doi.org/10.1016/j.ijms.2017.03.008.

(37) Marchand, A.; Rosu, F.; Zenobi, R.; Gabelica, V. Thermal Denaturation of DNA G-Quadruplexes and Their Complexes with Ligands: Thermodynamic Analysis of the Multiple States Revealed by Mass Spectrometry. *J. Am. Chem. Soc.* **2018**, *140* (39), 12553–12565. https://doi.org/10.1021/jacs.8b07302.

(38) Pruška, A.; Marchand, A.; Zenobi, R. Novel Insight into Proximal DNA Domain Interactions from Temperature-Controlled Electrospray Ionization Mass Spectrometry. *Angew. Chem. Int. Ed.* **2021**, *60* (28), 15390–15398. https://doi.org/10.1002/anie.202016757.

(39) Liu, J.; Wang, Y.; Wang, X.; Qin, W.; Li, G. Measuring Protein Unfolding Thermodynamic Stability in One Minute with Digital Temperature Control-Equipped nanoESI-Mass Spectrometry. *Int. J. Mass Spectrom.* **2023**, *494*, 117151. https://doi.org/10.1016/j.ijms.2023.117151.

(40) Daneshfar, R.; Kitova, E. N.; Klassen, J. S. Determination of Protein−Ligand Association Thermochemistry Using Variable-Temperature Nanoelectrospray Mass Spectrometry. *J. Am. Chem. Soc.* **2004**, *126* (15), 4786–4787. https://doi.org/10.1021/ja0316972.

(41) Raab, S. A.; El-Baba, T. J.; Woodall, D. W.; Liu, W.; Liu, Y.; Baird, Z.; Hales, D. A.; Laganowsky, A.; Russell, D. H.; Clemmer, D. E. Evidence for Many Unique Solution Structures for Chymotrypsin Inhibitor 2: A Thermodynamic Perspective Derived from vT-ESI-IMS-MS Measurements. *J. Am. Chem. Soc.* **2020**, *142* (41), 17372–17383. https://doi.org/10.1021/jacs.0c05365.

(42) Woodall, D. W.; Henderson, L. W.; Raab, S. A.; Honma, K.; Clemmer, D. E. Understanding the Thermal Denaturation of Myoglobin with IMS-MS: Evidence for Multiple Stable Structures and Trapped Pre-Equilibrium States. *J. Am. Soc. Mass Spectrom.* **2021**, *32* (1), 64–72. https://doi.org/10.1021/jasms.0c00075.

(43) Jordan, J. S.; Williams, E. R. Laser Heating Nanoelectrospray Emitters for Fast Protein Melting Measurements with Mass Spectrometry. *Anal. Chem.* **2022**, *94* (48), 16894–16900. https://doi.org/10.1021/acs.analchem.2c04204.

(44) Laszlo, K. J.; Buckner, J. H.; Munger, E. B.; Bush, M. F. Native-Like and Denatured Cytochrome *c* Ions Yield Cation-to-Anion Proton Transfer Reaction Products with Similar Collision Cross-Sections. *J. Am. Soc. Mass Spectrom.* **2017**, *28* (7), 1382–1391. https://doi.org/10.1007/s13361-017-1620-4.

(45) Leney, A. C.; Heck, A. J. R. Native Mass Spectrometry: What Is in the Name? *J. Am. Soc. Mass Spectrom.* **2017**, *28* (1), 5–13. https://doi.org/10.1007/s13361-016-1545-3.

(46) El-Baba, T. J.; Raab, S. A.; Buckley, R. P.; Brown, C. J.; Lutomski, C. A.; Henderson, L. W.; Woodall, D. W.; Shen, J.; Trinidad, J. C.; Niu, H.; Jarrold, M. F.; Russell, D. H.; Laganowsky, A.; Clemmer, D. E. Thermal Analysis of a Mixture of Ribosomal Proteins by vT-ESI-MS: Toward a Parallel Approach for Characterizing the Stabilitome. *Anal. Chem.* **2021**, *93* (24), 8484–8492. https://doi.org/10.1021/acs.analchem.1c00772.

(47) Giles, K.; Ujma, J.; Wildgoose, J.; Pringle, S.; Richardson, K.; Langridge, D.; Green, M. A Cyclic Ion Mobility-Mass Spectrometry System. *Anal. Chem.* **2019**, *91* (13), 8564–8573. https://doi.org/10.1021/acs.analchem.9b01838.

(48) Aune, K. C.; Salahuddin, A.; Zarlengo, M. H.; Tanford, C. Evidence for Residual Structure in Acid- and Heat-Denatured Proteins. *J. Biol. Chem.* **1967**, *242* (19), 4486–4489. https://doi.org/10.1016/S0021-9258(18)99563-3.

(49) Haezebrouck, P.; Joniau, M.; Van Dael, H.; Hooke, S. D.; Woodruff, N. D.; Dobson, C. M. An Equilibrium Partially Folded State of Human Lysozyme at Low pH. *J. Mol. Biol.* **1995**, *246* (3), 382–387. https://doi.org/10.1006/jmbi.1994.0093.

(50) Tanford, C.; Aune, K. C.; Ikai, A. Kinetics of Unfolding and Refolding of Proteins: III. Results for Lysozyme. *J. Mol. Biol.* **1973**, *73* (2), 185–197. https://doi.org/10.1016/0022-2836(73)90322-7.

(51) Kuwajima, K.; Hiraoka, Y.; Ikeguchi, M.; Sugai, S. Comparison of the Transient Folding Intermediates in Lysozyme and .Alpha.-Lactalbumin. *Biochemistry* **1985**, *24* (4), 874–881. https://doi.org/10.1021/bi00325a010.

(52) Kiefhaber, T. Kinetic Traps in Lysozyme Folding. *Proc. Natl. Acad. Sci.* **1995**, *92* (20), 9029–9033. https://doi.org/10.1073/pnas.92.20.9029.

(53) Kotov, V.; Mlynek, G.; Vesper, O.; Pletzer, M.; Wald, J.; Teixeira-Duarte, C. M.; Celia, H.; Garcia-Alai, M.; Nussberger, S.; Buchanan, S. K.; Morais-Cabral, J. H.; Loew, C.; Djinovic-Carugo, K.; Marlovits, T. C. In-Depth Interrogation of Protein Thermal Unfolding Data with MoltenProt. *Protein Sci.* **2021**, *30* (1), 201–217. https://doi.org/10.1002/pro.3986.

(54) Van Berkel, G. J.; Asano, K. G.; Schnier, P. D. Electrochemical Processes in a Wire-in-a-Capillary Bulk-Loaded, Nano-Electrospray Emitter. *J. Am. Soc. Mass Spectrom.* **2001**, *12* (7), 853–862. https://doi.org/10.1016/S1044-0305(01)00264-1.

(55) Gadzuk-Shea, M. M.; Hubbard, E. E.; Gozzo, T. A.; Bush, M. F. Sample pH Can Drift during Native Mass Spectrometry Experiments: Results from Ratiometric Fluorescence Imaging. *J. Am. Soc. Mass Spectrom.* **2023**, *34* (8), 1675–1684. https://doi.org/10.1021/jasms.3c00147.

(56) Savitzky, Abraham.; Golay, M. J. E. Smoothing and Differentiation of Data by Simplified Least Squares Procedures. *Anal. Chem.* **1964**, *36* (8), 1627–1639. https://doi.org/10.1021/ac60214a047.

(57) Creighton, T. E. The Energetic Ups and Downs of Protein Folding. *Nat. Struct. Biol.* **1994**, *1* (3), 135–138. https://doi.org/10.1038/nsb0394-135.

(58) Gozzo, T. A.; Weir, C. J.; Constabel, M. A.; Bush, M. F. Selecting Reducing Agents for Native Mass Spectrometry. ChemRxiv February 1, 2024. https://doi.org/10.26434/chemrxiv-2024-2nmh4-v2.

(59) Duckworth, H. W.; Nguyen, N. T.; Gao, Y.; Donald, L. J.; Maurus, R.; Ayed, A.; Bruneau, B.; Brayer, G. D. Enzyme–Substrate Complexes of Allosteric Citrate Synthase: Evidence for a Novel Intermediate in Substrate Binding. *Biochim. Biophys. Acta BBA - Proteins Proteomics* **2013**, *1834* (12), 2546–2553. https://doi.org/10.1016/j.bbapap.2013.07.019.

(60) Bai, J.-H.; Wang, H.-J.; Liu, D.-S.; Zhou, H.-M. Kinetics of Thermal Inactivation of Lactate Dehydrogenase from Rabbit Muscle. *J. Protein Chem. 16* (8).

APPENDIX A

Supplemental Information for Chapter III

Description of ptESI Source

The source design incorporates a Peltier thermoelectric chip (ATE1-TC-71-7R8A, Analog Technologies Inc) which moves heat to and from a small copper block placed on top of it. A thermistor (MP-3022, TE Technologies) is placed in the copper block to monitor the block temperature. A temperature controller (TC-720, TE Technologies) adjusts the voltage being supplied by an external DC power supply (72-420, Tenma) to the Peltier based on the measured block temperature. Thermal connections are made using thermal paste (NT-H1, Noctua). A hole has been drilled through the copper block, in which a borosilicate nESI capillary (1.00 mm outer diameter, 0.78 mm inner diameter) is placed. A 3D-printed acrylonitrile butadiene styrene clamp maintains even pressure on the Peltier and provides support for a platinum wire. The source is mounted on a xyz stage (PI, Auburn, MA) on a rail carriage (XT66P2/M, Thor Labs) for easy positioning in front of an instrument inlet. A render of the source is shown in Figure S1.

A customized program is used to set the desired starting, incubation (optional), high, low, and ending temperatures; scan rate(s), waveform, and number of cycles for each experiment. The source is currently set to operate between 5 – 95 °C. Incubation steps can be programmed for any desired length of time. The scan rate can be changed between program steps (Fig. S2).

Discussion of Disulfide Scrambling

A past study noted that high charge states apparent in the high temperature mass spectra appear similar to spectra in which disulfide scrambling has occurred.[1] If disulfide scrambling is occurring at elevated temperatures, the protein would be locked in an unfolded state during the cooling phase of the thermal cycle and the mass spectra at low temperatures would have the same charge state distribution as the high-temperature spectra. Inspection of the mass spectra from thermal cycling (Fig. S3) shows that this is not the case, and the low temperature spectra at the end of the cycle resemble those from the beginning of the experiment. This is also reflected in the average charge state returning to its low initial value at the end of the thermal cycle. It seems unlikely that disulfide scrambling is occurring. High charge state peaks are present with low intensity at low temperatures, even before thermal cycling, and these are likely due to other degradation events.

Equation S1

Sigmoidal curve fitting is performed using the equation below:

$$\bar{z} = \frac{L}{1 + e^{-k(x - x_0)}} + b$$

where $\bar{z}$ is the average charge state, x is the block temperature, x_0 is the midpoint temperature, and L, b, and k are fitting parameters.

Table S1. T_m values for thermal cycles of lysozyme in Figure 5.

	Cycle 1 Heat	**Cycle 1 Cool**	**Cycle 2 Heat**	**Cycle 2 Cool**	**Cycle 3 Heat**	**Cycle 3 Cool**
T_m (°C)	55.7	47.0	56.7	47.3	55.4	46.3

The T_m values show a large difference between those obtained from the heating phase and those obtained from the cooling phase. There are decreases changes in T_m as the number of cycles increases. The magnitude of the change varies between runs, as the calculation of T_m is linked to fluctuations in ion current. As discussed previously, T_m is not a solid metric to evaluate changes between cycles.

Table S2. T_m values for three thermal cycles of lysozyme as shown in Figure 6.

Rate	**Cycle 1 Heat**	**Cycle 1 Cool**	**Cycle 2 Heat**	**Cycle 2 Cool**	**Cycle 3 Heat**	**Cycle 3 Cool**
9 °C·min^{-1}	53.0	47.7	52.0	46.8	51.5	45.8
15 °C·min^{-1}	52.0	43.6	51.5	43.1	51.4	42.0
30 °C·min^{-1}	54.1	39.4	54.5	38.9	54.7	38.4

The T_m values for the cooling phase decrease more significantly than those for the heating phase, across all scan rates investigated.

Table S3. T_m values for three thermal cycles of lysozyme as shown in Figure 7.

	Cycle 1 Heat	**Cycle 1 Cool**	**Cycle 2 Heat**	**Cycle 2 Cool**	**Cycle 3 Heat**	**Cycle 3 Cool**
T_m (°C)	69.9	60.0	66.6	59.2	64.9	58.5

The T_m values obtained from the multiplexed experiment (pH 2.15) are higher than those obtained for other cycling experiments (pH 2.0) shown in this study.

Table S4. T_m values for 10 thermal cycles on lysozyme as shown in Figure S7.

Cycle Number	Tm Heat (°C)	Tm Cool (°C)
1	63.7	52.2
2	66.1	51.8
3	64.2	48.0
4	64.0	50.1
5	64.4	48.0
6	60.7	45.4
7	62.5	46.9
8	62.7	46.7
9	63.1	47.4
10	63.8	49.0

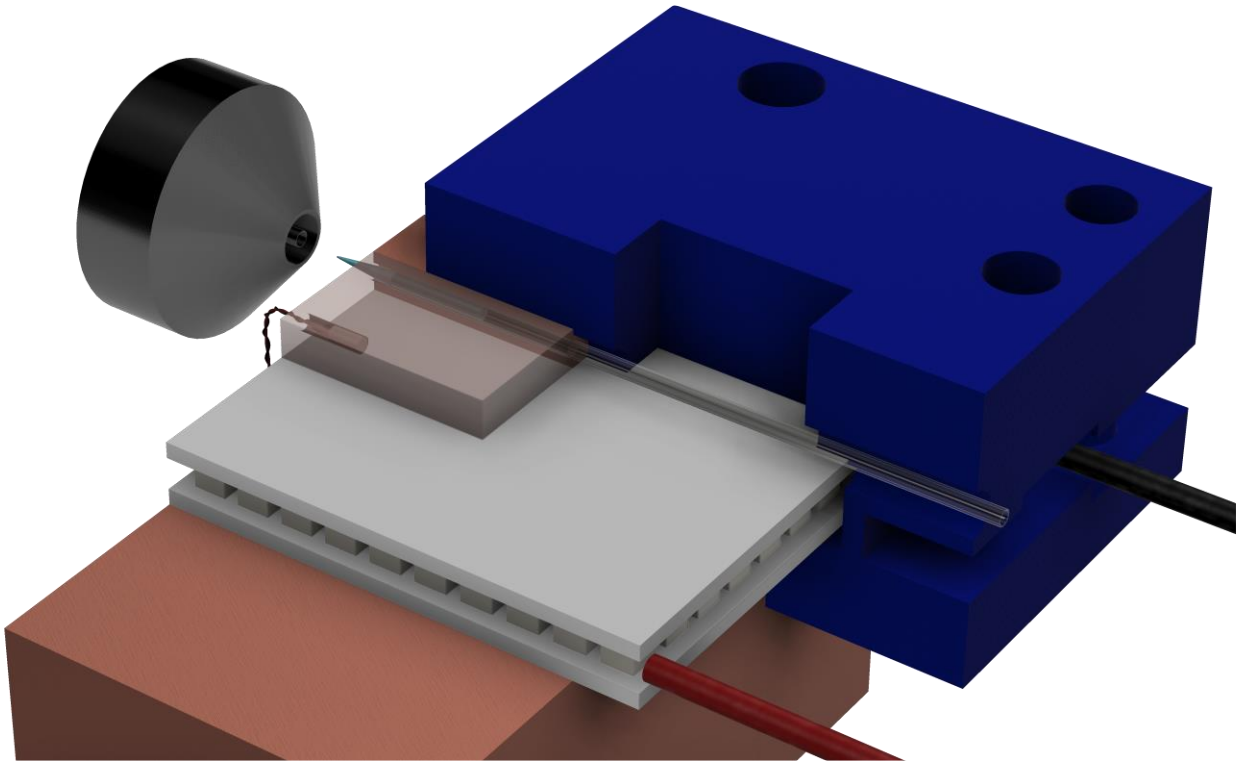

Figure S1. Render of the ptESI source depicting the Peltier, copper block, embedded thermistor, nESI capillary and 3D-printed clamp in front of an instrument inlet.

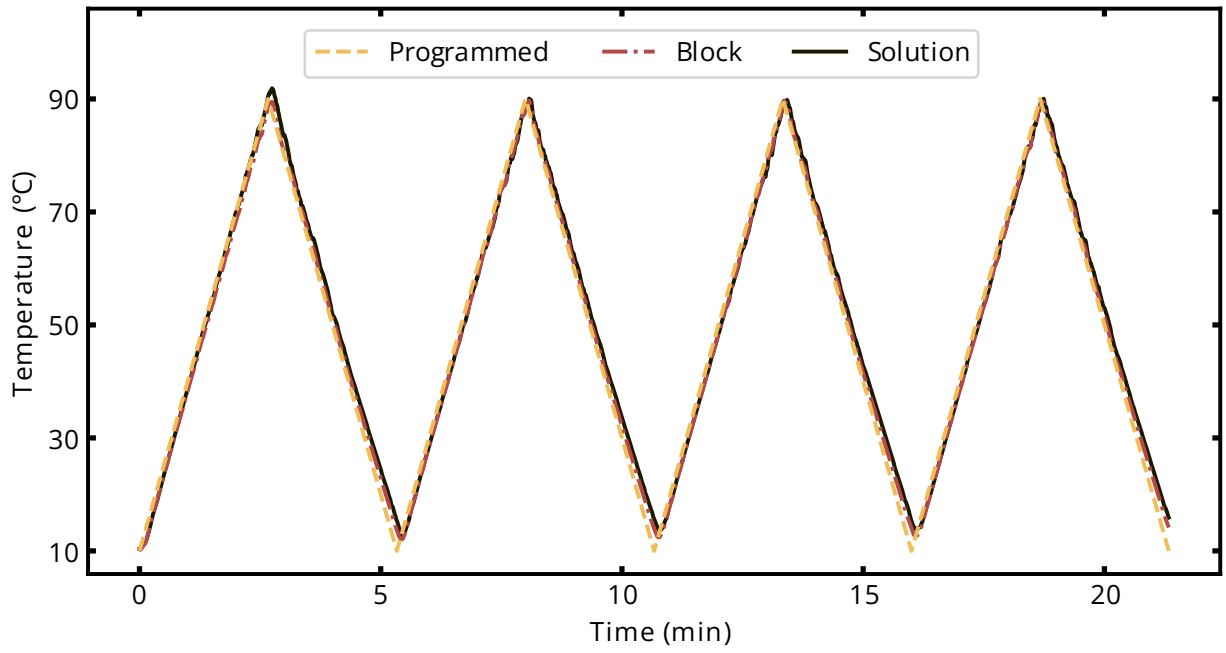

Figure S2. Characterization data for the ptESI source showing four thermal cycles of 10 – 90 – 10 °C at 30 °C.min^{-1} in 21.3 minutes. The programmed (yellow), block (red), and solution (black) temperatures are in close agreement throughout the experiment; thus the block temperature is used as a proxy for the solution temperature.

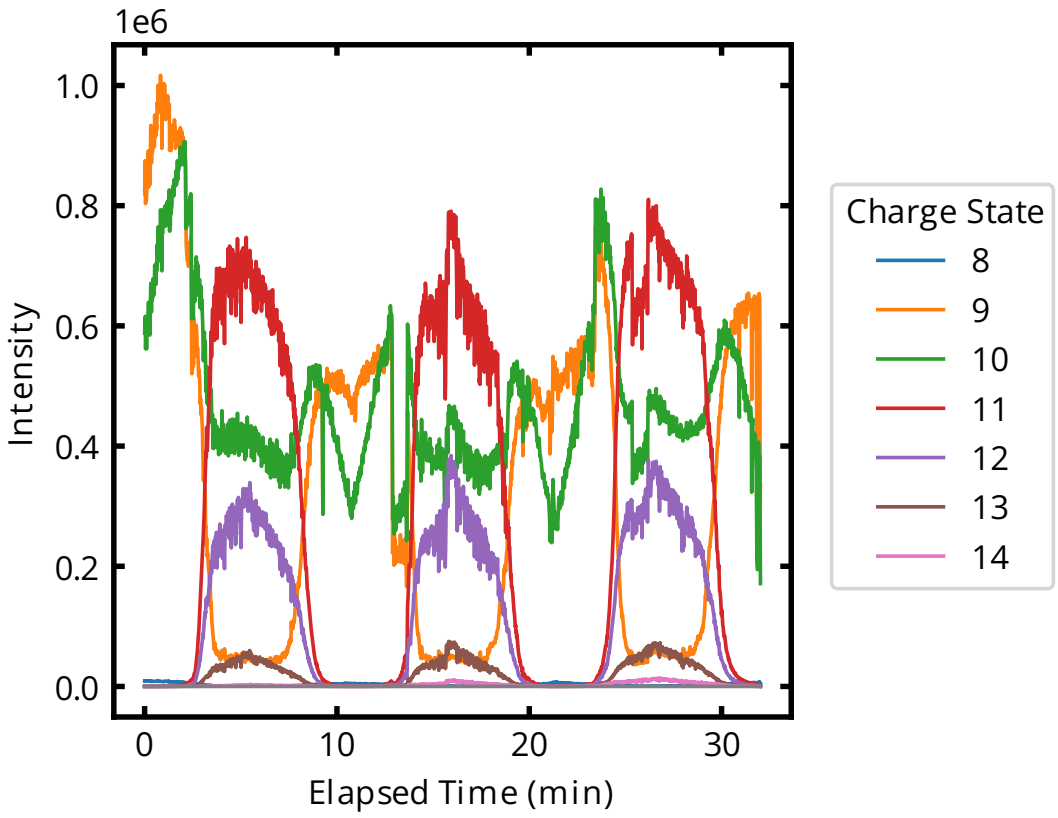

Figure S3. Extracted ion chromatogram for lysozyme data shown in Figure 5. It shows the ion chromatogram that has been extracted from the total ion chromatogram for each charge state. The mass ranges for each charge state as set by the analyst.

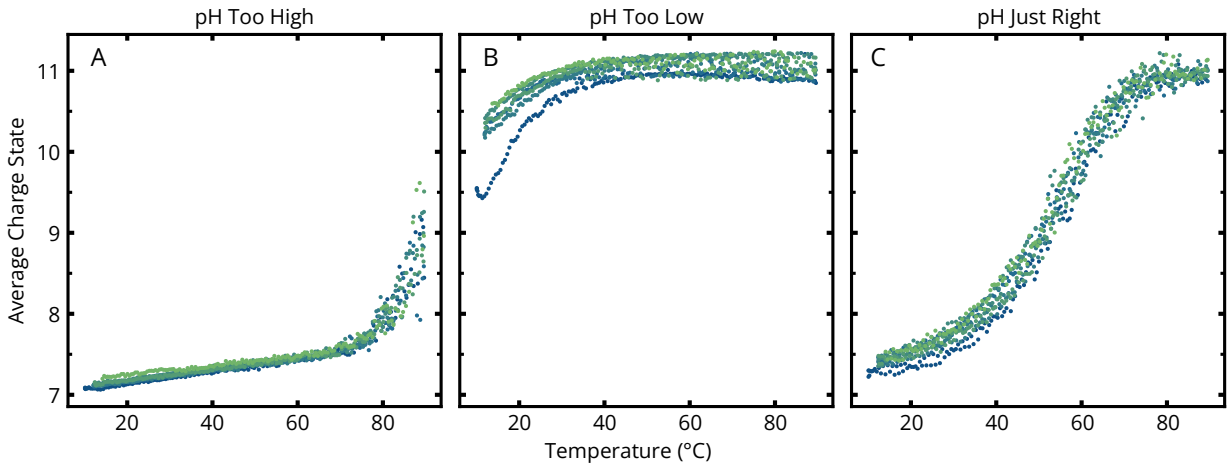

Figure S4. Ubiquitin is highly sensitive to small changes in pH. When the pH is too high (A), only the bottom asymptotic region of the sigmoidal curve is visible. When the pH is too low (B), the curve is shifted the other direction and only the upper asymptotic region is visible. Careful control of solution pH is required to capture the sigmoidal curve (C). These data do not have a precise measurement, as they predate our lab's micro pH electrode.

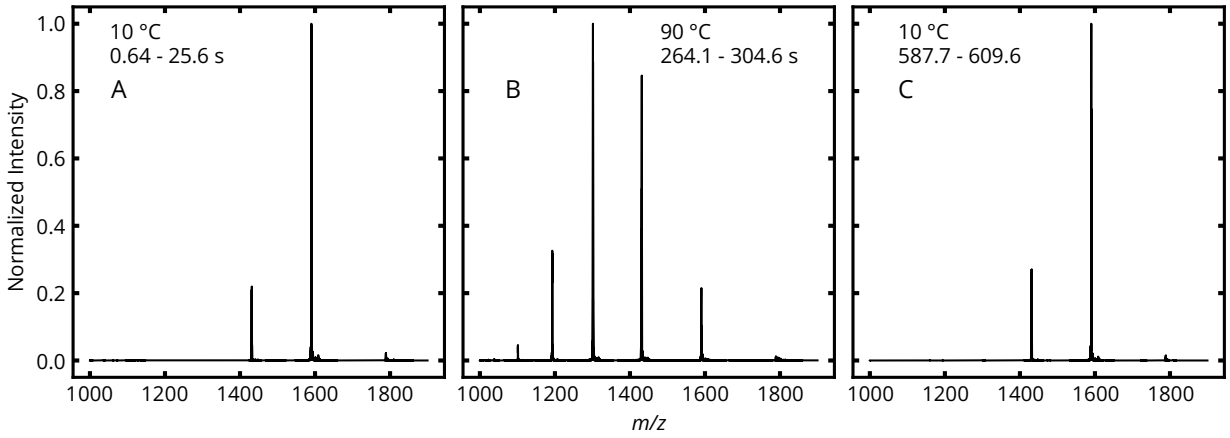

Figure S5. Mass spectra of lysozyme from a thermal cycle. A) At low temperatures at the beginning of the cycle, lysozyme is folded and the charge state distribution shown, with lower average charge state. B) At high temperatures in the middle of the cycle, lysozyme is unfolded and the charge state distribution shifts to higher values. C) At low temperatures at the end of the cycle, the charge state distribution shifts back to the initial state as lysozyme refolds. If disulfide scrambling were occurring, we would expect the final low temperature spectrum to have the same charge state distribution as at high temperature. As this is not the case and the unfolding is reversible, it seems unlikely that disulfide scrambling is occurring.

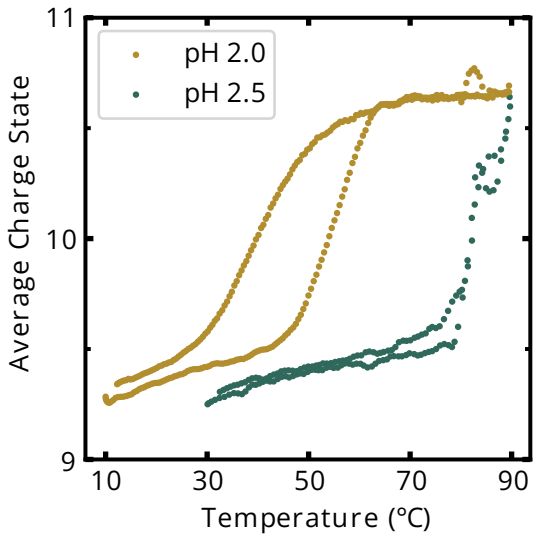

Figure S6. The T_m values for lysozyme depend strongly on pH. At pH 2.0, the values of T_m for unfolding and refolding are 54.1 and 39.4 °C, respectively. At pH 2.5, the resulting curve is unable to be fit to a sigmoidal curve, but the value of T_m can be estimated as ~85 °C. The T_m shifts ~ 38 °C higher over only 0.5 pH units.

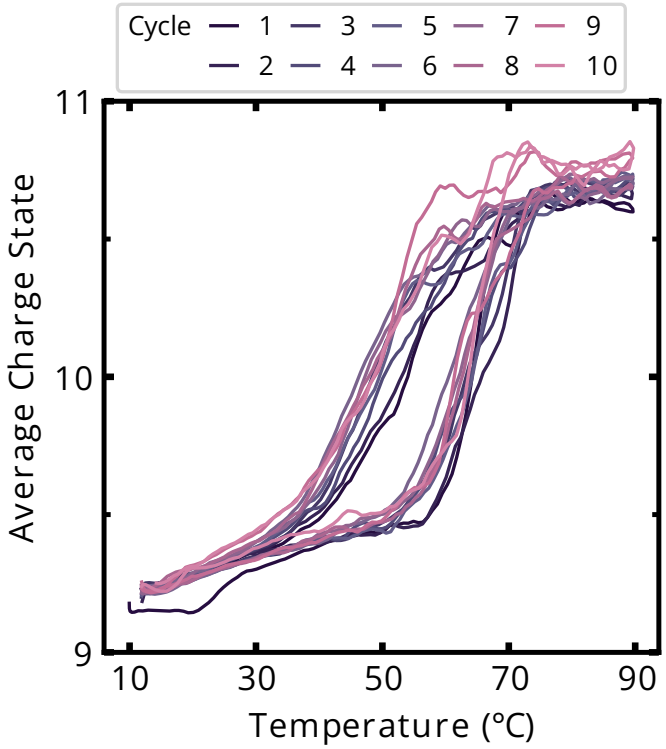

Figure S7. Lysozyme is cycled at the fastest scan rate, ±30 °C·min^{-1}, for the duration of the slowest scan rate experiment, 50 min. This 10-cycle experiment demonstrates the stability of lysozyme and the reversibility of its unfolding. The T_m initially shifts to lower temperatures as the number of cycles increases, but then appears to shift back. This may be due to fluctuations in the ion current. The values of Tm are shown in Table S4 and are plotted in Figure S8. The minor transition at low temperatures during the first heating phase may be the irreversible loss of a structural feature or a kinetically trapped state resulting from freezing. Further experiments are planned.

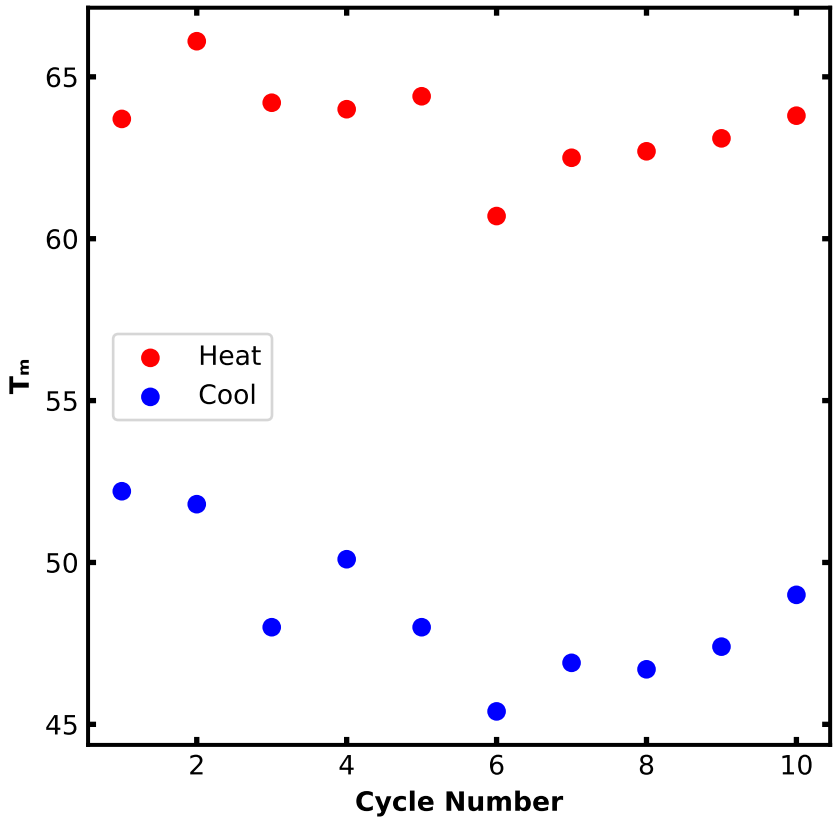

Figure S8. Values of T_m from the 10-cycle experiment (Fig. S7) are plotted. The values from the heating phases (red) appear to be more stable than those from the cooling phase (blue). However, as discussed previously, T_m is not an ideal metric for comparing between cycles within the same experiment.

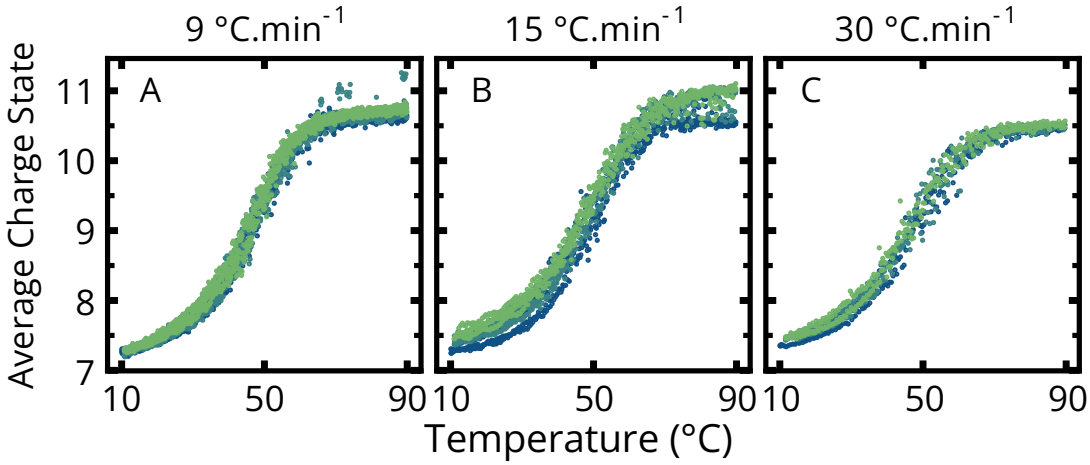

Figure S9. Three thermal cycles of ubiquitin at three different scan rates. A) Three cycles at ±9 °C·min^{-1}. The average T_m is 45.5 ± 0.9 °C. B) Three cycles at ±15 °C·min^{-1}. The average T_m is 47.5 ± 1.2 °C. C) Three cycles at ±30 °C·min^{-1}. The average T_m is 45.8 ± 1.3 °C. There are no significant differences between the curves at the three different scan rates.

References

(1) Wang, G.; Abzalimov, R. R.; Kaltashov, I. A. Direct Monitoring of Heat-Stressed Biopolymers with Temperature-Controlled Electrospray Ionization Mass Spectrometry. *Anal. Chem.* **2011**, *83* (8), 2870–2876. https://doi.org/10.1021/ac200441a.